Bezafibrate activation of PPAR drives oxidative stress, glutathione depletion and cellular maladaptation in VLCAD deficiency

Martin Lund[1], Kathrine G. Andersen[1], Robert Heaton[2], Iain P. Hargreaves[2], Niels Gregersen[1], Rikke K. J. Olsen[1]

[1]Research Unit for Molecular Medicine, Department of Clinical Medicine, Aarhus University and Aarhus University Hospital, Brendstrupgaardsvej 100, 8200, Aarhus, Denmark

[2]School of Pharmacy, Liverpool John Moore University, Byrom Street, Liverpool L3 3AF, United Kingdom

Correspondence:

Rikke K. J. Olsen

Research Unit for Molecular Medicine, Aarhus University Hospital,

Palle Juul-Jensens Boulevard 99, 8200 Aarhus, Denmark

E-mail: rikke.olsen@clin.au.dk

Highlights

- Our findings further implicate disruption of redox homeostasis in VLCAD deficiency
- Chronic PPAR overactivation is a plausible initiator of the pathogenic process
- Glutathione depletion indicate a broader role for thiols in VLCAD deficiency

Author contributions

All authors contributed to the project design and final manuscript. In addition:

M.L.: wrote the draft paper, planned the project, and performed the majority of the assays and data analysis.

K.G.A.: performed part of the image cytometry, qPCR, western blotting, and associated data analysis.

R.H. & I.H.: supervised spectrophotometric assays and guided data analysis.

N. G. & R. K. J. O planned and supervised the project and revised the draft manuscript.

Conflicts of interest

The study was partially funded by Ultragenyx Pharmaceutical Inc., without influence on project design.

Keywords

Mitochondria, glutathione, thiols, bezafibrate, PPAR, oxidative stress, ROS, VLCAD, VLCAD deficiency, inborn errors of metabolism, fatty acids oxidation deficiency.

Total words in numbered sections:	6416
Word in abstracts:	246
No. of figures:	13
No. of tables:	1
Supplementary data:	
No. of figures:	5
No. of tables:	1

ABSTRACT

Very long-chain acyl-CoA dehydrogenase (VLCAD) deficiency is the most common inborn long-chain fatty acid oxidation (FAO) disorder. VLCAD deficiency is characterized by distinct phenotypes. The severe phenotypes are potentially life-threatening and affect the heart or liver, with a comparatively milder phenotype characterized by myopathic symptoms. There is an unmet clinical need for effective treatment options for the myopathic phenotype. The molecular mechanisms driving the gradual decrease in mitochondrial function and associated alterations of muscle fibers are unclear.

The peroxisome proliferator-activated receptor (PPAR) pan-agonist bezafibrate is a potent modulator of FAO and multiple other mitochondrial functions and has been proposed as a potential medication for myopathic cases of long-chain FAO disorders. *In vitro* experiments have demonstrated the ability of bezafibrate to increase VLCAD expression and activity. However, the outcome of small-scale clinical trials has been controversial.

We found VLCAD deficient patient fibroblasts to have an increased oxidative stress burden and deranged mitochondrial oxidative phosphorylation capacity, compared to controls. Applying heat stress under fasting conditions to bezafibrate pretreated patient cells, caused a marked further increase of mitochondrial superoxide levels. Patient cells failed to maintain levels of the essential thiol peptide antioxidant glutathione and experienced a decrease in cellular viability. Our findings indicate that chronic PPAR activation is a plausible initiator of long-term pathogenesis in VLCAD deficiency. Our findings further implicate disruption of redox homeostasis as a key pathogenic mechanism in VLCAD deficiency and support the notion that a deranged thiol metabolism might be an important pathogenic factor in VLCAD deficiency.

1. Introduction

Very long-chain acyl-CoA dehydrogenase (VLCAD) deficiency was first described in 1993 [1]. As the most common of the inborn long-chain fatty acid oxidation (FAO) disorders, VLCAD deficiency is clinically well-described and is part of neonatal screening programs in many countries [2]. The enzymatic function of VLCAD is to catalyze the initial step of mitochondrial β-oxidation. VLCAD can process long-chain fatty acids with chain lengths from 12 to 22 carbons, with each β-oxidation cycle removing two carbons [3]. The worst phenotypes are characterized by ATP homeostasis failure that in the most severe cases results in death. FAO is a major contributor to the energy requirements of several tissues, especially so for the heart and liver [4, 5]. The most severe phenotypes do indeed involve the heart or liver respectively and are associated with episodes of hypoketotic hypoglycemia, risk of multi-organ failure, and sudden death [6-8]. A comparatively milder skeletal muscle phenotype is associated with myalgia, hypotonia, and rhabdomyolysis [6-8]. The most severe phenotype is typically associated with biallelic loss-of-function variations, resulting in very low residual enzymatic capacity. For the missense variations, associated with milder myopathic phenotypes, there is less predictability with regard to genotype-phenotype relationships [7, 9].

In general, patients are intolerant of physical stress, such as extended fasting or exercise, fever, and temperature extremes [6]. During such events, there is a metabolic shift towards a dependency upon FAO in some tissues and a consequent inability to maintain ATP levels, due to inborn reduced FAO capacity. In addition, external thermal stress or increased internal heat production associated with increased mitochondrial activity can disrupt protein complexes that associate with mutated or absent VLCAD protein, such as the respiratory chain supercomplexes, and thereby potentially further decreasing FAO capacity [10, 11]. While the acute symptoms during physical stress are well explained by failure to maintain ATP levels in affected tissues, several aspects of disease progression over time are not well understood.

The milder myopathic form has characteristics of being an acquired rather than solely an inborn disorder, inasmuch as it can take decades for sufficient cellular dysfunction to develop and give rise to symptoms [2, 6, 12]. Dysfunctional cellular traits include reduced mitochondrial quality, e.g. development of secondary respiratory chain deficiency and maladaptive muscle fiber

bioenergetic/metabolic shifts [10, 13-16]. Pathogenic factors (apart from ATP homeostasis failure) that could lead to reduced mitochondrial quality and cellular dysfunction include substrate and metabolite accumulation ("lipotoxicity"), co-factor sequestration and cellular stress imposed by misfolded or absent protein, but their relative importance is not known [17]. Biochemical findings in VLCAD deficient patients include accumulation of characteristic acyl-carnitines [15, 18], as well as non-specific indicators of mitochondrial stress, such as increased levels of reactive oxygen species (ROS) [16, 17, 19-21]. Some of these pathogenic factors are functionally connected, for instance, coenzyme A (CoA) attachment via a thiol bond is required for transport and oxidation of long-chain fatty acids, and insufficient long-chain FAO rates can thus lead to sequestration of the essential cofactor CoA [22].

From a clinical perspective, dampening chronic stressors such as excessive ROS, may reduce the negative selective pressure on the mitochondrial population as a whole and lead to a reduction or reversal of disease progression. The most important antioxidant systems for mitochondrial redox homeostasis is superoxide dismutase 1 and 2 and the tripeptide glutathione (GSH), along with enzymes associated with GSH function [23]. A well-functioning mitochondrial oxidative phosphorylation (OXPHOS) system is necessary for maintaining matrix NADPH levels, which in turn powers recycling of oxidized mitochondrial GSH (GSSG). It has been suggested that because GSH is only produced in the cytosol and is subsequently imported into the mitochondria, dysfunctional mitochondria with high ROS production and insufficient capacity for NADPH production can potentially function as GSH/thiol sinks [23].

Currently, therapy is based on dietary intervention and supplementation, leaving an unmet need for effective pharmacological therapies [17]. Over the past decade, bezafibrate has emerged as a possible pharmacological therapy candidate for treating biochemically mild cases of long-chain FAO disorders; including VLCAD deficiency [24] and carnitine palmitoyltransferase 2 (CPT2) deficiency [25]. Interpreting the results of small-scale clinical trials has proven controversial, but it is safe to conclude that bezafibrate has not been globally adopted as an effective treatment option [26-31]. The fibrate family is well-known as agonists of the different peroxisome proliferator-activated receptors (PPAR) isoforms. Two of these isoforms (PPARα

and PPARδ) are central regulators of cellular lipid metabolism. Bezafibrate acts as both a PPARα and PPARδ agonist with similar potency [32]. Activation of these isoforms leads to an increased fatty acid transport into the mitochondria and increased mitochondrial capacity for β-oxidation [32]. Since the basic theoretical foundation of bezafibrate treatment and *in vitro* results are impeccable, it is important to investigate the possible mechanisms that have resulted in the lack of clear clinical success, so that these can be surmounted in the future.

The PPARs and their activation of the signaling protein PPAR-γ coactivator 1α (PGC-1α) together induce overall biogenesis and activity of mitochondria and other cellular systems. This includes increased expression of mitochondrial OXPHOS proteins and increased expression of the inducible antioxidants, such as SOD1, SOD2, catalase and GSH [33-36]. While this potentially could be beneficial in mitochondrial disorders, the outcome of this increased biogenesis depends on the overall quality of the mitochondria produced [37, 38]. Indeed, part of the bezafibrate controversy is that chronic PPAR(α) overactivation in long-chain FAO disorders has been proposed as an important long-term pathogenic mechanism [39, 40]. Forced PPAR(α) induced biogenesis of dysfunctional mitochondria might constitute a pathway for reducing mitochondrial quality over time, by exceeding the capacity of the mitophagy system to remove damaged mitochondria. As damaged mitochondrial fragments accumulate and fuse with functional mitochondria these in turn become dysfunctional due to disruption of cristae structure, increased ROS levels, depolarization of the inner membrane, etc. [38, 41, 42].

In the present study, we investigated whether PPAR activation via bezafibrate treatment would affect not only the mitochondrial FAO system but also the redox balance and overall OXPHOS capacity in VLCAD deficient cells and thereby alter their tolerance to energy requiring metabolic stress over time.

2. Methods

2.1. Patient and control dermal fibroblasts

Dermal fibroblast cells derived from six patients, diagnosed with VLCAD deficiency based on clinical presentation, abnormal acyl-carnitines, and biallelic pathogenic VLCAD variations were included in the study. VLCAD deficient dermal fibroblast cell lines were anonymized as per the instructions of the Danish National Committee on Health Research Ethics. The anonymized VLCAD deficient cell lines were subsequently assigned abbreviations, as seen in table 1. Commercial control dermal fibroblast cell lines (Control 1 – Control 6) was abbreviated as C1-C6. Control dermal fibroblast vendor information is listed in supplementary data.

Patients	Abbreviation	*ACADVL* genotype
Mild phenotype patient 1	**M1**	p.[Val243Ala];[Val243Ala]
Mild phenotype patient 2	**M2**	p.[Thr190Ile];[LOF]
Mild phenotype patient 3	**M3**	p.[Val243Ala];[LOF]
Severe phenotype patient 1	**S1**	p.[LOF];[LOF]
Severe phenotype patient 2	**S2**	p.[LOF];[LOF]
Severe phenotype patient 3	**S3**	p.[LOF];[LOF]

Table 1.

Patient *ACADVL* genotypes and study ID.

*LOF: loss of function variants, incl. premature termination codons and variants in canonical splice sites.

2.2. Cell culturing & heat stress model

The human dermal fibroblast cell lines were cultured in Minimum Essential Media (MEM) (Lonza) supplemented with 5 mM L-glutamine (Sigma), 10%v/v fetal bovine serum (Invitrogen), and 0.1%v/v penicillin & streptomycin (Sigma) under standard conditions in a CO_2 incubator. MEM has glucose concentrations equivalent to serum glucose after overnight fasting (1g/l). Fibroblasts used for assays were kept below 14 passages and were routinely checked for mycoplasma. Djouadi, F. *et al.* originally demonstrated that bezafibrate increases long-chain FAO capacity in mild cases of CPT2 and VLCAD deficiency, findings which since have been replicated and expanded to other long-chain FAO disorders [24, 25, 43, 44]. Even though bezafibrate does not increase VLCAD expression in biochemically severe VLCAD deficient cells, we still included three severe phenotype patients, because we were interested in general disease mechanisms that over time can drive the alteration in mitochondrial function observed

in patients [15, 45]. Bezafibrate-induced increase in expression levels of VLCAD plateaus after 48 hours treatment with 400 µM bezafibrate in mild VLCAD deficient fibroblasts [25]. In order to allow sufficient time for the individual cell-lines to adapt to bezafibrate-induced alterations of protein expression patterns, baseline measurements of the effect of bezafibrate were performed after 96 hours of incubation with either 0 µM or 400 µM bezafibrate (Sigma), with media renewal every 24 hours [24, 25].

Bezafibrate was initially solubilized in dimethylsulfoxide DMSO (Sigma); final DMSO concentration in media was 0,002%v/v. Cell pellets for polymerase chain reaction, western blotting, and spectrophotometry assays were harvested and stored at -80°C after 96 hours of (pre)treatment. *In vitro* investigation of the effects of bezafibrate on cellular redox balance was performed before and after the application of stress, because stress induced symptoms is a major part of the clinical presentation. The decision to applying heat stress *in vitro* was based partly on its clinical relevance as described in the introduction and partly because application of heat stress further improves the predictive power of the *in vitro* long-chain FAO flux assay, which is the current prognostic gold standard for VLCAD deficiency, indicating that this is a relevant stressor to apply *in vitro* [6, 11, 46-48].

For the fasting heat stress assay, cells were pretreated in the manner described above for 96 hours and subsequently subjected to heat stress (41°C) for 24, 48, 72, 96 or 120 hours, without further renewal of media. For all assays, cells were reseeded after the first 72 hours of initial treatment, so that all experiments could be performed at approximately 80-90% culture confluence (Fig. 1).

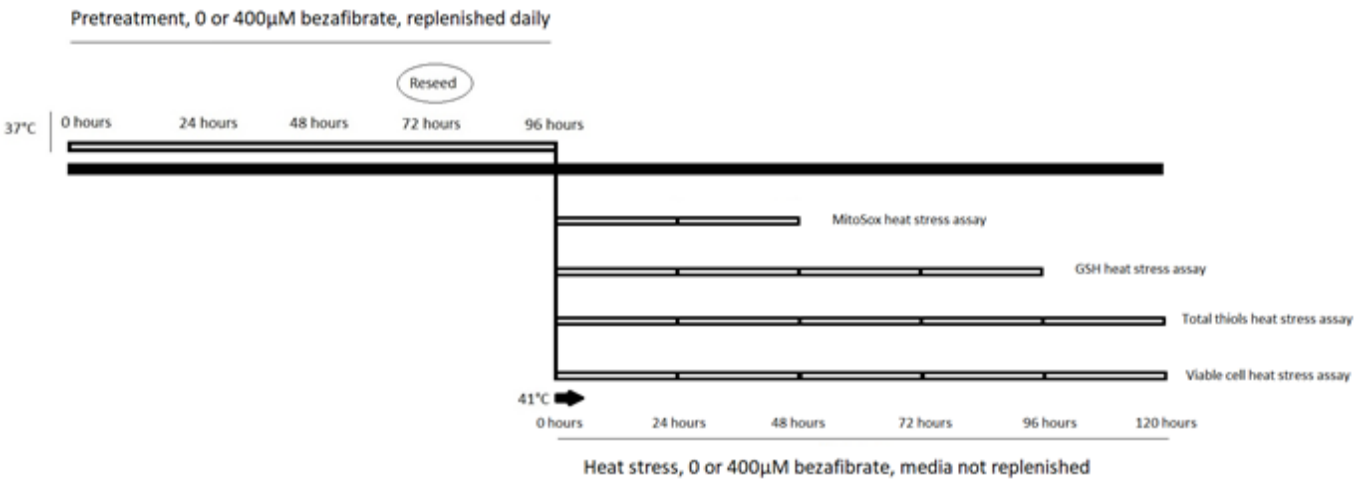

Fig. 1. Experimental Setup

Illustrates experimental procedure for cell culture treatment prior to and during fasting heat stress. Cells were pretreated with either 0 µM or 400 µM bezafibrate for a total of 96 hours. At this point, baseline measurements were performed (t=0 hours). Media during pretreatment was replenished every 24 hours and cells were reseeded after 72 hours of bezafibrate treatment. During heat stress, the culture media was not replenished. Vertical lines along the assay bars indicate at what time points the different assays were performed during heat stress.

2.3. Reverse transcription quantitative polymerase chain reaction

Reverse transcription quantitative polymerase chain reaction (RT-qPCR) procedure was modified from previously published procedures [49, 50]. Total RNA was isolated from thawed fibroblast pellets using TRIzol® Reagent (Ambion, Life Technologies) and isolated RNA was treated with DNAse free (Ambion, Life Technologies) to remove any remaining DNA contamination. Only RNA samples that showed no apparent degradation when subjected to denaturing gel electrophoresis and with an A260/A280 ratio above 1.8 were used (Nanodrop 1000, Thermo Fischer Scientific). Complementary DNA (cDNA) was synthesized from 1µg RNA using iScript cDNA synthesis kit (Bio-Rad) with a mixture of random hexamer and oligo (dT) primers, in accordance with the manufacturer's instructions. Measurement of mRNA levels was performed with TaqMan assays (Invitrogen) specific for *ACADVL* or *ACTB* (Applied Biosystems; Hs00825606_g1 and 4310881E) in triplicates by quantitative real-time PCR according to the manufacturer's instructions and using the StepOne Plus detection system (Applied Biosystems). Relative gene expression was calculated by the "standard curve method", and the expression of *ACADVL* normalized to the expression of the endogenous beta-actin control gene, *ACTB*.

2.4. Western blotting

Western blotting assay was performed in a modified form of previously published procedures [51]. Thawed fibroblast pellet was lysed via probe sonication on ice. Lysis buffer was composed of 1 M Urea with 200 mM ammonium bicarbonate (Sigma) and supplemented with Complete™ mini protease inhibitor cocktail (Roche). Total protein was measured by Bradford assay (Bio-Rad). 25 µg protein total cell lysate was loaded on Criterion™ TGX Stain-Free™ any kD gels (Bio-Rad) and blotted to low fluorescence PVDF membranes (Bio-Rad) on a TransBlot® Turbo™ (Bio-Rad) transfer system. Criterion™ TGX Stain-Free™ gels contain trihalo compounds that, after activation with UV-light, reacts with tryptophan and creates covalently bound fluorophores. The fluorophores are used to quantify whole lane protein and is superior to using so-called household proteins for normalization and loading control [52]. The membranes were blocked, washed, and probed with primary antibody against VLCAD (MitoScience, MC1488) overnight. Subsequently, membranes were washed and probed with horseradish peroxidase-conjugated goat anti-rabbit secondary antibodies(DAKO), which was detected by enhanced

chemiluminescence (ECL) Plus detection kit (Amersham Biosciences), using the ImageQuant LAS 4000 (GE Healthcare) detection system.

2.5. Spectrophotometric enzyme assays

Spectrophotometric measurement of enzyme activity and sample protein concentration was performed on an Uvikon XS spectrometer following previously published procedures [53]. All enzyme activity measurements were carried out at 37°C, with sufficient substrate present to saturate the relevant enzymatic systems. Citrate synthase (CS) catalyzes the condensation of oxaloacetate and acetyl-CoA to citrate and CoA. Enzyme activity was measured at 412 nm using Ellman's reagent (5 5'-dithiobis- 2-nitrobenzoic acid), acetyl-CoA, oxaloacetate, and a Tris/Triton buffer [54]. The calculated activity was normalized to total protein concentration, measured by Lowry assay [55]. Mitochondrial respiratory chain complex I catalyze NADH oxidation, electrons are transferred from NADH through complex I to ubiquinone, which is then reduced to ubiquinol. The complex I inhibitor rotenone allows the deduction of non-complex I specific activity [56, 57]. The activity was measured at 340 nm in a potassium phosphate buffer. Both CS and complex I activity can be used as markers of mitochondrial density in healthy populations [53, 58]. Mitochondrial respiratory chain complex II/III activity is measured by supplying succinate for oxidation by complex II, thereby passing electrons into a ubiquinone pool, producing ubiquinol. This, in turn, reduces cytochrome C in a reaction catalyzed by complex III. Antimycin A sensitive activity was measured at 550 nm in a potassium phosphate buffer [57, 59]. All reagents were purchased from Sigma.

2.6. Image cytometry

The image cytometry utilized here follows procedures described previously in Fernandez-Guerra et al. [19]. All image cytometry assays were performed on a NucleoCounter 3000 using A2-slides (ChemoMetec). Data were gated and analyzed with NucleoView™ software (ChemoMetec).

2.6.1. Image cytometry reagents

40,60-Diamidino-2-phenylindole (DAPI), acridine orange (AO), propidium iodide (PI), Hoechst 33342 (Hoechst), VitaBright43 (glutathione/GSH), Vitabright48 (reduced total thiols) and cell counting assay lysis buffer was purchased from ChemoMetec. Antimycin, trypsin solution,

phosphate buffered saline (PBS), bezafibrate, l-buthionine sulphoximine (BSO) and dimethylsulfoxide (DMSO) were purchased from Sigma-Aldrich. Hanks balanced salt solution (+Ca & Mg) and MitoSOX Red mitochondrial superoxide probe (MitoSOX) were purchased from Invitrogen. RedDot2 was purchased from Biotium. DAPI fluorescence was detected using peak excitation at 365 nm and emission at 470/55. Vitabright43 and Vitabrigth48 fluorescence were detected using peak excitation at 365 nm and emission at 470/55 nm. Reddot2 fluorescence was detected at peak excitation 630 nm and emission at 740/60 nm. AO fluorescence was measured at peak excitation 475 nm, and emission at 560/35 nm. PI fluorescence was measured at peak excitation of 530 nm and emission at 675/75 nm. The Hoechst fluorescence was detected using peak excitation at 365 nm and emission at 470/55 nm, MitoSOX at 475 nm and emission at 675/75 nm. When seeding cells, total and viable cells were measured by analyzing fibroblasts in solution immediately after the addition of DAPI for non-viable cell concentration and with the addition of lysis buffer for total cell concentration.

2.6.2. Glutathione and total reduced thiols levels

Vitabright43 and Vitabright48 are cell permeable dye that reacts with intracellular thiol groups forming a fluorescent compound [60, 61]. Total thiol measurement with trypsinized cells was performed by addition of Vitabrigth48, PI, and AO (20, 25 and 0.06 mg/mL, respectively). PI functions as a dead cell identifier and AO for identification of individual nuclei and thus individual cells. Glutathione (GSH) measurement with trypsinized cells was performed by addition of Vitabrigth43. RedDot2 was used as a dead cell stain, and the NucleoCounter3000 Darkfield option was used to identify individual cells. Reddot2 was used at a total 1:1000 dilution to detect dead cells and Vitabright43 at 1:200 final dilution. As a positive control, we inhibited the rate-limiting step of GSH synthesis for 16 hours using 0.5 mM l-buthionine sulphoximine (BSO), which removed the majority of the GSH probe (Vitabrigt43) signal as previously described [61]. The chosen GSH probe has the great advantage that unlike the conventional GSH probes such as monochlorobimane, the Vitabright probes are not enzyme dependent [61].

2.6.3. Mitochondrial superoxide level

Prior to the assay, Hanks balanced salt solution containing 150 mM antimycin A was added to a cell culture well containing an untreated control fibroblast cell line (C1) and incubated at 37°C for 5 minutes, as a positive control for MitoSOX labeling. Hanks balanced salt solution containing 5 mM MitoSOX was added to each assay well and incubated for 20 min at 37°C. Fibroblasts were trypsinized, washed and incubated with 10 mg/mL Hoechst for 15 min at 37°C in order to identify individual cells and subsequently stained with the dead cell stain RedDot2 as above, after which samples was immediately loaded and analyzed.

2.7. Statistical analysis

The spectrophotometric, western blot, and RT-qPCR data is based on samples prepared from two or more independent cultures of each cell line. The presented image cytometry data is from at least three independent cultures of each individual cell line. Image cytometry and PCR assays were performed with n=6 control and n=6 patient dermal fibroblast cell lines. Western blotting and spectrophotometric analysis assays were performed with n=3 control and n=6 patient dermal fibroblast cell lines. Excel was used for final statistical analysis using paired or unpaired t-test as appropriate and for calculating the standard deviation (SD) or standard error for the mean (SEM). P-values < 0.05 were considered significant. For baseline measurements, paired t-tests were used for the same cell lines with or without bezafibrate. For heat stress assays, paired tests were used for the same cell line and bezafibrate concentration, at different durations of heat stress. Calculation of SD, SEM and statistical tests was performed in Microsoft Excel.

3. Results

The present study aimed at investigating the effect of bezafibrate treatment on cellular redox response and viability in VLCAD deficient cells before and after external stress. The study design is depicted in Fig. 1. A series of baseline measurements of mitochondrial function was performed at the equivalent of t=0 hours of fasting heat stress, followed by measurements of changes in redox associated parameters at 24-hour intervals during fasting heat stress.

3.1. The effect of bezafibrate on VLCAD expression at baseline

As expected, bezafibrate treatment increases VLCAD gene transcription in the VLCAD deficient patient fibroblasts (Fig. 2A) and VLCAD protein expression levels in cells from patients with biochemically mild VLCAD deficiency (Fig. 2B). Treatment did not increase VLCAD protein levels in patient fibroblasts with the severe clinical phenotype, as they all carry biallelic loss-of-function variations.

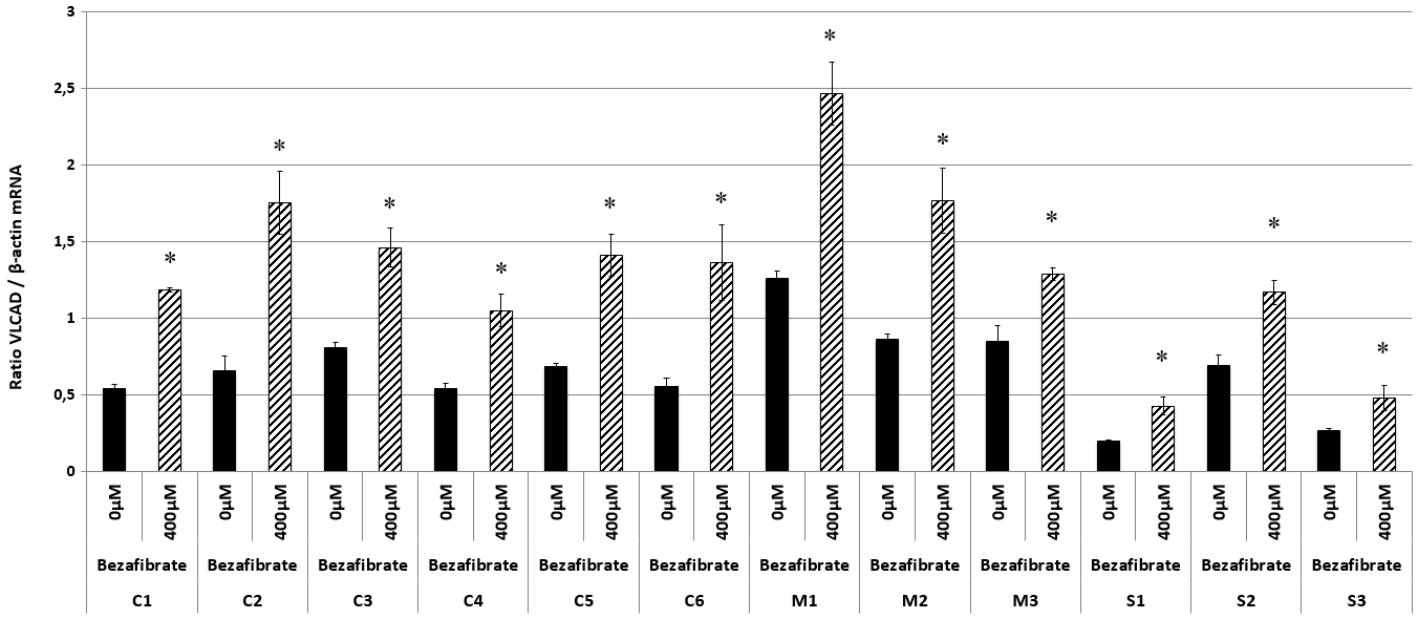

Fig. 2A. VLCAD/β-actin mRNA ratio

The graph shows the ratio of VLCAD mRNA to β-actin mRNA for the six individual control or VLCAD deficient dermal fibroblasts cell lines. These were treated with either 0 µM (solid bars) or 400 µM (dashed bars) bezafibrate for 96 hours. Error bars represent the standard deviation from two independent cultures. Paired t-test for 0 µM versus 400 µM bezafibrate for the individual dermal fibroblasts cell lines * $p<0.05$. Controls 1-6 are abbreviated as C1-C6. Mild phenotype patients 1-3 are abbreviated as M1-3. Severe phenotype patients 1-3 are abbreviated as S1-3.

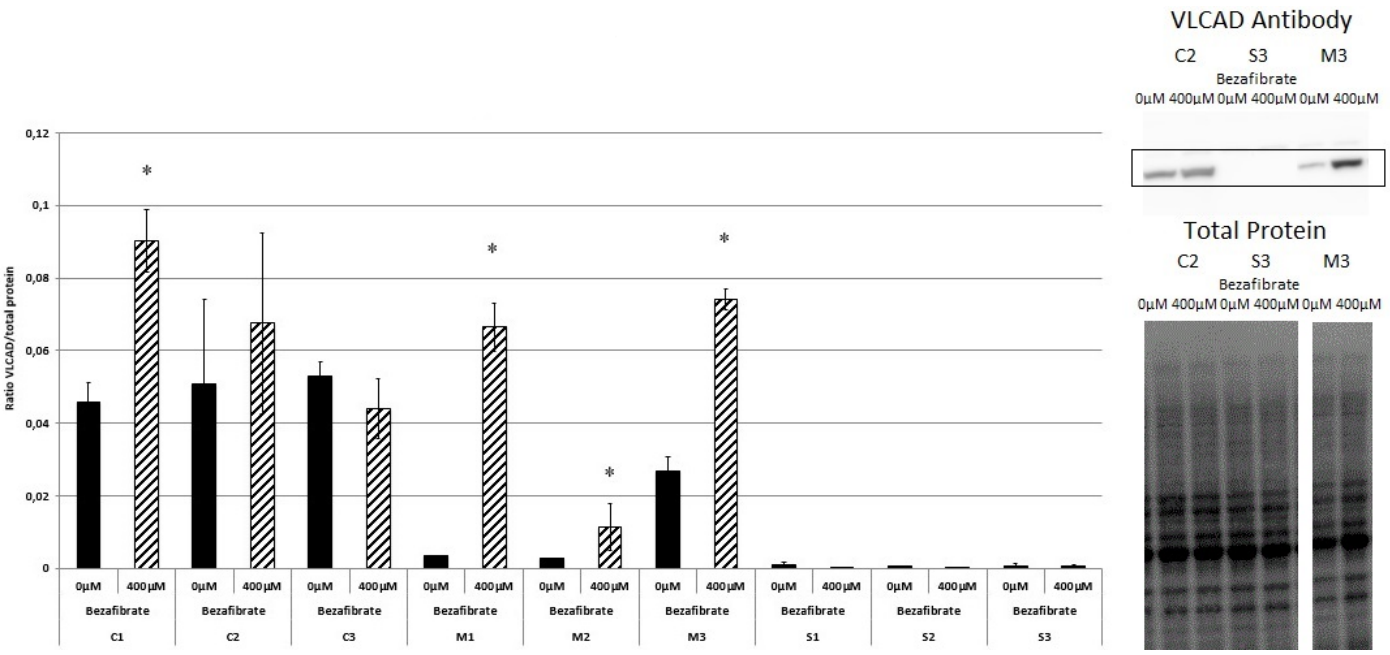

Fig. 2B. VLCAD/whole lane total protein ratio

The graph shows enhanced chemiluminescence based detection of VLCAD antibody binding, normalized to whole lane total protein, detected with a tryptophan-trihalo fluorophore. Graph bars shows six individual control or VLCAD deficient dermal fibroblasts cell lines (left) and representative examples of VLCAD protein and whole lane total protein detection (right). Cells were treated with either 0 µM (solid bars) or 400 µM (dashed bars) bezafibrate for 96 hours. Error bars represent the standard deviation from two independent cultures. Paired t-test for 0 µM versus 400 µM bezafibrate for the individual dermal fibroblasts cell lines * $p<0.05$. Controls 1-3 are abbreviated as C1-C3. Mild phenotype patients 1-3 are abbreviated as M1-3. Severe phenotype patients 1-3 are abbreviated as S1-3.

3.2. The effect of bezafibrate on mitochondrial superoxide levels at baseline

As previously mentioned, a significant oxidative stress burden has been observed in VLCAD deficiency [19-21]. Comparing control and VLCAD deficient dermal fibroblasts, we found significantly increased levels of mitochondrial superoxide (Fig. 3). Treatment with 400 µM bezafibrate did not significantly alter mitochondrial superoxide levels in either controls or patients compared to 0 µM bezafibrate. Levels of superoxide did not correlate with the severity of the genotype, see Fig. S1A for a plot of individual cell lines.

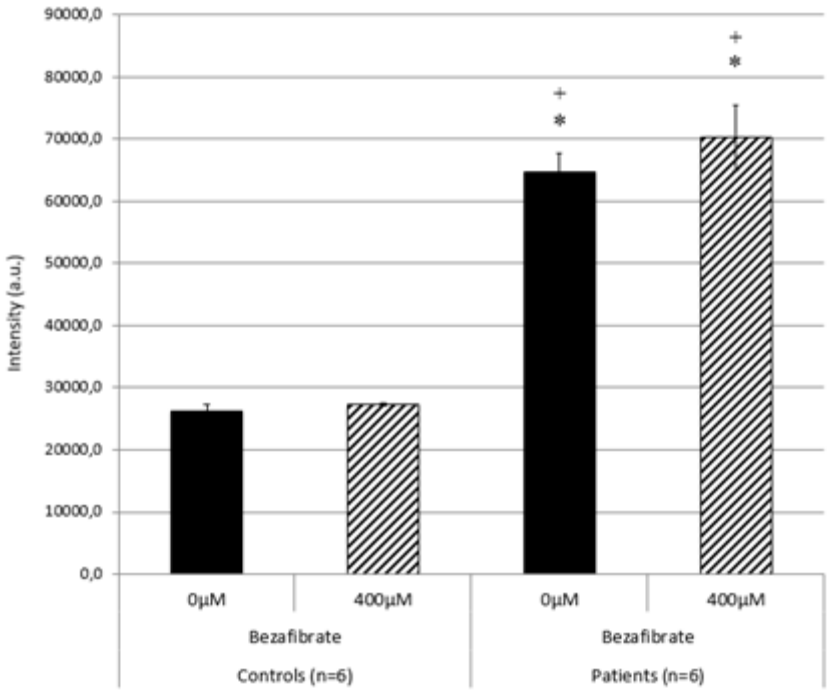

Fig. 3. MitoSox probe intensity

The graph shows MitoSox probe mean intensity (a.u.) for six control or VLCAD deficient dermal fibroblasts cell lines. These were treated either with 0 µM (solid bars) or 400 µM (dashed bars) bezafibrate for 96 hours. Error bars represent SEM, data from 3(+) independent cultures. Significant p-values ($p<0.05$) are indicated as: *$p<0.05$ for control fibroblasts treated with 0 µM bezafibrate versus other experimental conditions, $^{+}p<0.05$ for control fibroblasts treated with 400 µM bezafibrate versus remaining experimental conditions.

3.3. The effects of bezafibrate on mitochondrial metabolism at baseline

VLCAD deficient patients suffer from an inborn mitochondrial FAO deficiency, but can also develop secondary dysfunctions in other metabolic systems, such as in the mitochondrial respiratory chain [10, 15]. The respiratory chain is a major contributor to total cellular ROS, which is produced as a byproduct of its essential role in maintaining cellular ATP levels. Additionally, the respiratory chain and Krebs cycle are responsible for maintaining sufficient NADPH levels in the mitochondrial matrix, which powers the mitochondrial antioxidant system [23]. This means that the mitochondrial metabolism simultaneously is a major contributor to and eliminator of oxidative damage [62, 63]. The effects of bezafibrate on the mitochondrial respiratory chain and Krebs cycle in VLCAD deficient cells was measured using spectrophotometry, specifically the activity of mitochondrial citrate synthase (CS), as well as

mitochondrial respiratory chain complex I and complex II/III activities was measured in control and patient fibroblast lysates.

Untreated patient cells had significantly higher complex I activity per milligram protein, compared to untreated control cells (Fig. 4A). 96 hours treatment with 400 µM bezafibrate led to a near doubling of complex I activity in controls, which as Fig. 3 shows, does not lead to a corresponding increase in control superoxide levels, despite complex I being a major source of mitochondrial superoxide [63]. The relative increase in complex I activity in patient cells after bezafibrate treatment was smaller compared to that observed in controls and reached a lower absolute amount (Fig. 4A).

Untreated patient cells had significantly higher complex II/III activity, compared to control cells (Fig. 4B). As with complex I, treatment with 400 µM bezafibrate led to a near doubling of complex II/III activity in control fibroblasts, compared to 0 µM bezafibrate. Again, this did not lead to a corresponding increase in leakage of electrons to form superoxide (Fig. 3). In contrast, patient cell treated with 400 µM bezafibrate experienced a decrease of complex II/III activity. The reaction of complex II/III to bezafibrate treatment is thus inverted in patient cells compared to controls. CS is the entry point of acetyl-CoA into the Krebs cycle and is thus a crucial participant in mitochondrial metabolism [64]. CS activity was significantly reduced in untreated patient cell lines compared to controls (Fig. 4C). Following 400 µM bezafibrate treatment, the patients CS activity levels were normalized to the equivalent of untreated control levels. In control cell lines, addition of 400 µM bezafibrate led to a significant increase in CS activity. Bezafibrate induced activation of PPARs will normally induce mitochondrial biogenesis [33]. The effect of bezafibrate on mitochondrial metabolic capacity in patient cells did not clearly correlate with genotype severity (Fig. S1B-S1D).

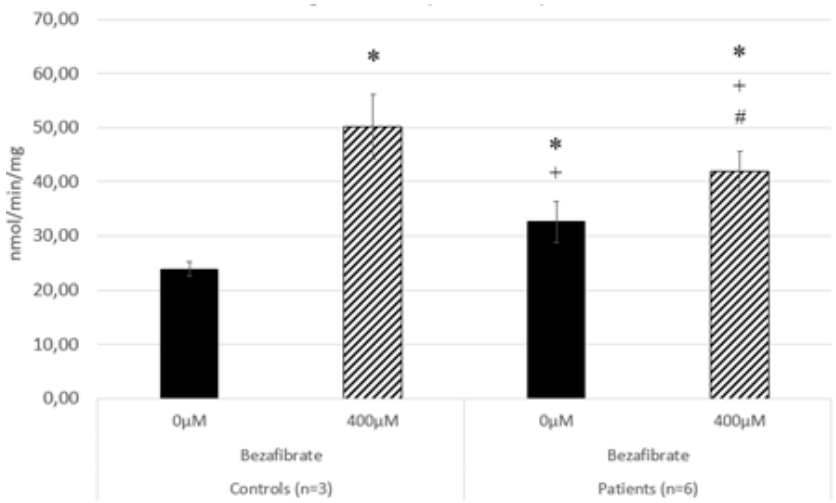

Fig. 4A. Complex I capacity

The graph shows the respiratory chain complex I mean maximum activity ((nmol/min)/mg protein) in three control and six VLCAD deficient dermal fibroblasts cell lines. These were treated either with 0 µM (solid bars) or 400 µM (dashed bars) bezafibrate for 96 hours. Error bars represent SEM, data from 2(+) independent cultures. Significant p-values ($p<0.05$) are indicated as: *$p<0.05$ for control fibroblasts treated with 0 µM bezafibrate versus other experimental conditions, $^{+}p<0.05$ for control fibroblasts treated with 400 µM bezafibrate versus remaining experimental conditions, $^{\#}p<0.05$ for patient fibroblasts treated with 0 µM bezafibrate versus remaining experimental condition.

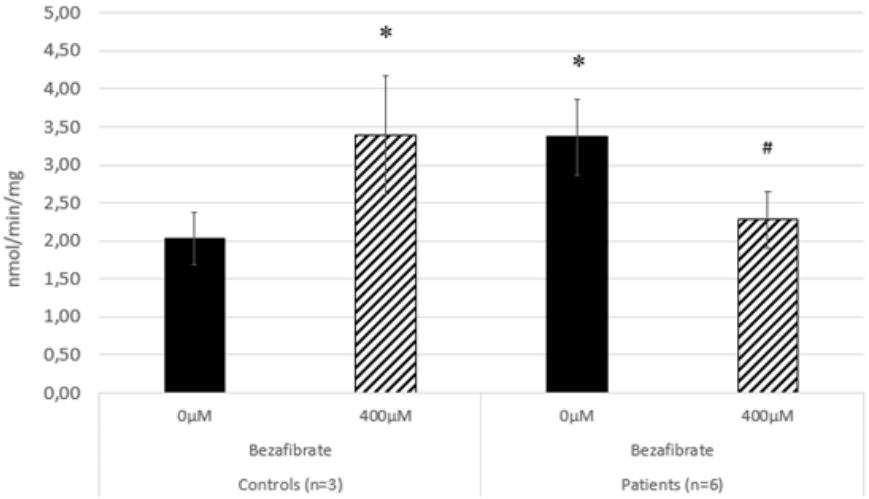

Fig. 4B. Complex II/III capacity

The graph shows respiratory chain complex II/III mean maximum activity ((nmol/min)/mg protein) in three control or six VLCAD deficient dermal fibroblasts cell lines. These were treated either with 0 µM (solid bars) or 400 µM (dashed bars) bezafibrate for 96 hours. Error bars represent SEM, data from 2(+) independent cultures. Significant p-values ($p<0.05$) are indicated as: *$p<0.05$ for control fibroblasts treated with 0 µM bezafibrate versus other experimental conditions.

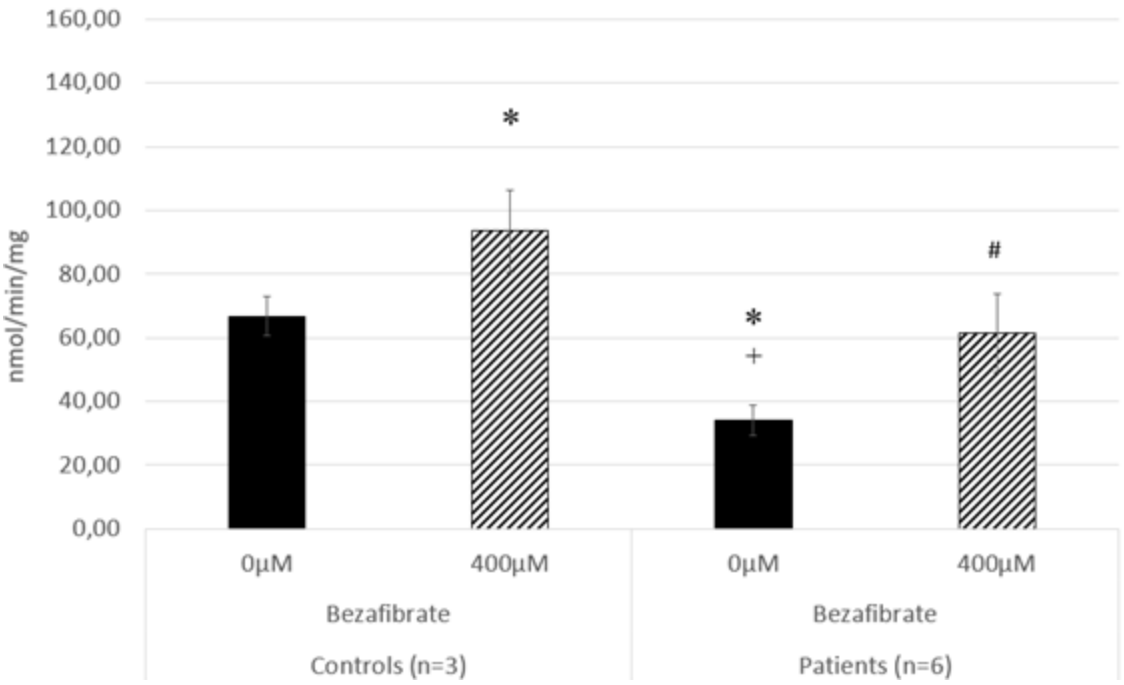

Fig. 4C. Citrate synthase capacity

The graph shows Krebs cycle enzyme citrate synthase mean maximum activity ((nmol/min)/mg protein) in three control or six VLCAD deficient dermal fibroblasts cell lines. These were treated either with 0 µM (solid bars) or 400 µM (dashed bars) bezafibrate for 96 hours. Error bars represent SEM, data from 2(+) independent cultures. Significant p-values ($p<0.05$) are indicated as: *$p<0.05$ for control fibroblasts treated with 0 µM bezafibrate versus other experimental conditions, $^{+}p<0.05$ for control fibroblasts treated with 400 µM bezafibrate versus remaining experimental conditions, $^{\#}p<0.05$ for patient fibroblasts treated with 0 µM bezafibrate versus remaining experimental condition.

3.4. The effects of bezafibrate on cellular GSH levels at baseline

Cells with VLCAD deficiency are subject to both an increased oxidative stress burden and dysregulation of metabolic systems that maintain the NAD(P)H pool in the mitochondria. Concurrently cellular CoA metabolism is stressed, as excessive intracellular accumulation of long-chain fatty acids attached via a thiol-bond to CoA will lead to sequestration of CoA [22, 65, 66]. The system composed of the thiol-containing tripeptide glutathione (GSH) and associated enzymes are ultimately responsible for the removal of ROS and oxidative damage, inside and adjacent to mitochondria [23]. Using a GSH specific probe (VitaBright43), as well as a pan-thiol targeted probe (VitaBright48), we found that both GSH and total thiols levels were increased in untreated patient cells compared to similarly untreated controls (Fig. 5A). The increased levels of GSH matches the higher oxidative burden measured in patients compared to controls (Fig. 3).

After 400 µM bezafibrate treatment, there was a slight but significant increase in total reduced thiol levels in controls, but not a significant increase in the patient cell lines (Fig. 5B). The GSH levels in patients treated with 400 µM bezafibrate were normalized to controls levels, but superoxide levels did not decrease correspondingly. Viewed individually, there was also no clear relationship between decreased GSH level in specific cell lines and levels of superoxide in the matrix after treatment with 400 µM bezafibrate (Fig. S1A & S1E).

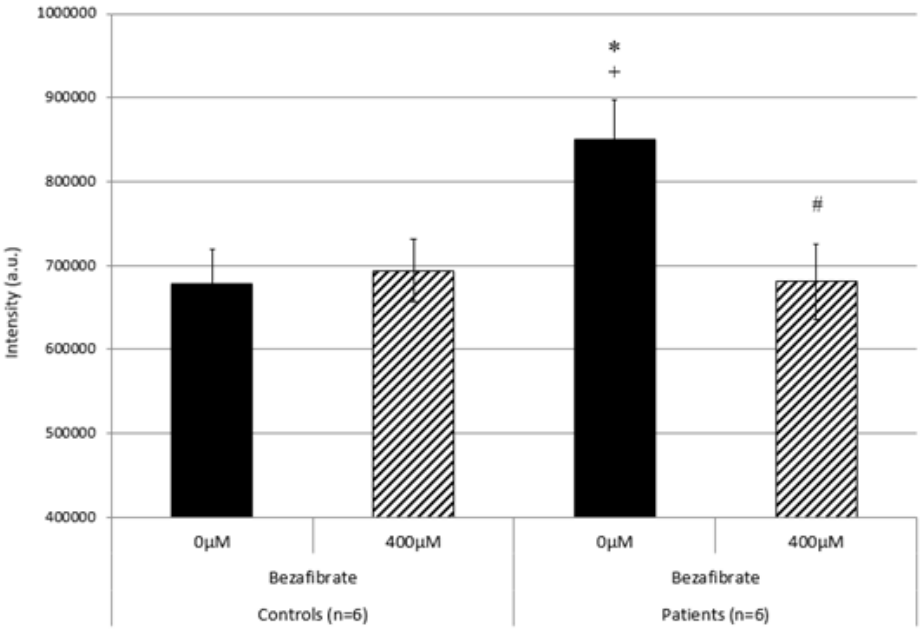

Fig. 5A. GSH probe intensity

The graph shows reduced GSH (VitaBright43) probe mean intensity (a.u.) for six control or VLCAD deficient dermal fibroblasts cell lines. These were treated either with 0 µM (solid bars) or 400 µM (dashed bars) bezafibrate for 96 hours. Error bars represent SEM, data from 3(+) independent cultures. Significant p-values ($p<0.05$) are indicated as: *$p<0.05$ for control fibroblasts treated with 0 µM bezafibrate versus other experimental conditions, $^{+}p<0.05$ for control fibroblasts treated with 400 µM bezafibrate versus remaining experimental conditions, $^{\#}p<0.05$ for patient fibroblasts treated with 0 µM bezafibrate versus remaining experimental condition.

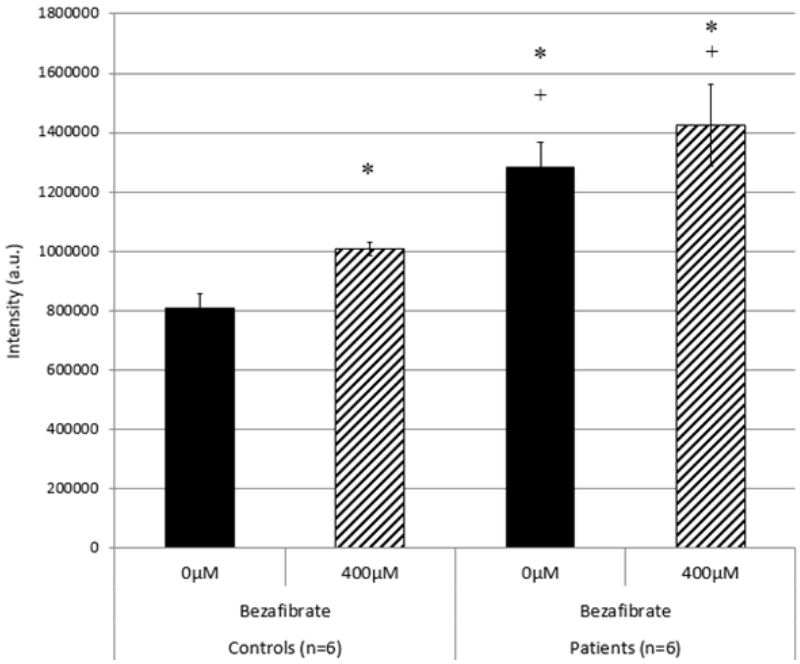

Fig. 5B. Total thiol probe intensity

The graph shows reduced total thiol (VitaBright48) probe mean intensity (a.u.) for six control or VLCAD deficient dermal fibroblasts cell lines. These were treated either with 0 µM (solid bars) or 400 µM (dashed bars) bezafibrate for 96 hours. Error bars represent SEM, data from 3(+) independent cultures. Significant p-values ($p<0.05$) are indicated as: *$p<0.05$ for control fibroblasts treated with 0 µM bezafibrate versus other experimental conditions, $^{+}p<0.05$ for control fibroblasts treated with 400 µM bezafibrate versus remaining experimental conditions.

3.5. Bezafibrate pretreatment increases mitochondrial ROS levels during heat stress

Manifestation of symptoms as a result of metabolic stress is an important aspect of VLCAD deficiency. Having completed the baseline measurements, we therefore proceeded to expose the control and patient fibroblasts cell lines to heat stress under fasting conditions. See materials and methods for the experimental setup. Mitochondrial superoxide levels were measured with the MitoSox probe after 24 and 48 hours of heat stress (Fig. 6). Whereas bezafibrate treatment did not increase mitochondrial superoxide levels at baseline, bezafibrate treatment during heat stress significantly increased mitochondrial superoxide levels in both control and patient cells. In patient cells, this occurred already after 24 hours of stress, whereas control cells required 48 hours of stress to reach significantly altered levels of superoxide. After 48 hours, the patient cell lines pretreated with 400 µM bezafibrate had significantly higher levels of superoxide than patient cell lines cultured without bezafibrate ($p=0.0026$).

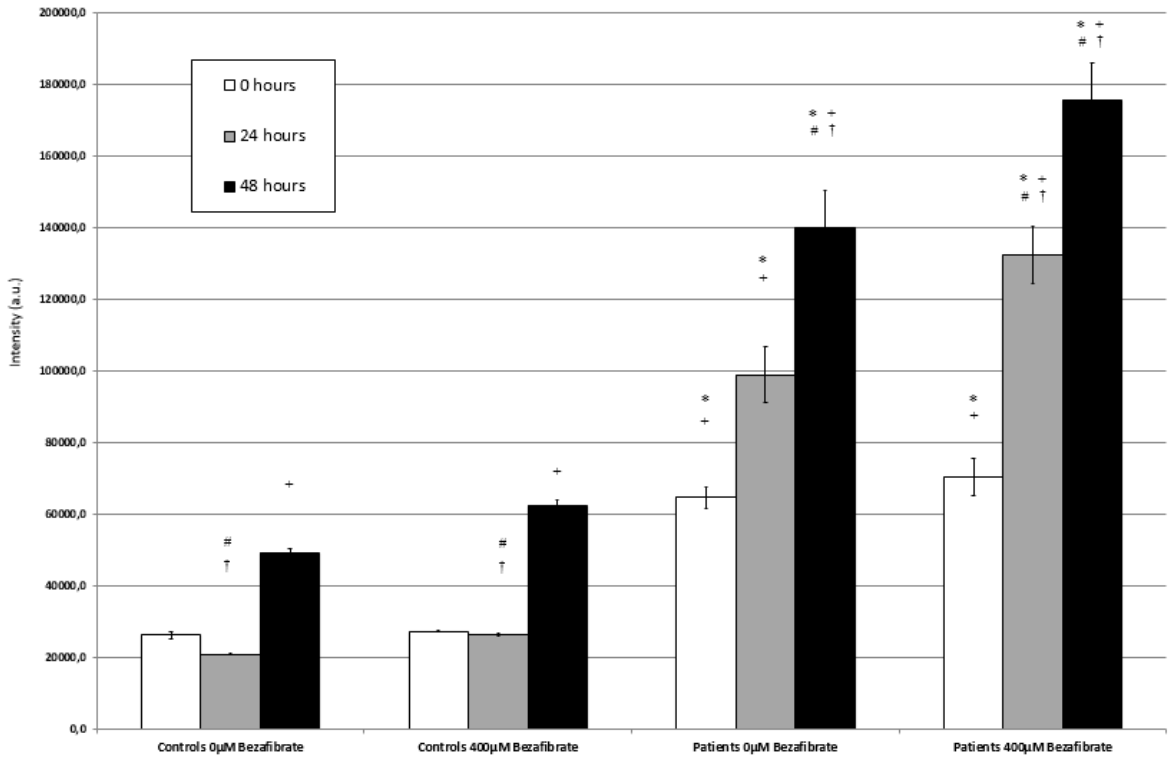

Fig. 6. MitoSox probe intensity during heat stress

The graph shows MitoSox probe mean intensity (a.u.) for six control or VLCAD deficient dermal fibroblasts cell lines. These were treated either with 0 µM or 400 µM bezafibrate for 96 hours. The pretreated cell lines were subsequently exposed to heat stress (41°C) for 0 hours (solid white), 24 hours (solid gray) or 48 hours (solid black). Error bars represent SEM, data from 3(+) independent cultures. Test of statistical significance is presented for the four experimental variables at baseline (heat stress = 0 hours), compared to remaining experimental conditions. Significant p-values ($p<0.05$) are indicated as: *$p<0.05$ for control fibroblasts treated with 0 µM bezafibrate at t=0 hours versus other experimental conditions, $^{+}p<0.05$ for control fibroblasts treated with 400 µM bezafibrate at t=0 hours versus remaining experimental conditions, $^{\#}p<0.05$ for patient fibroblasts treated with 0 µM bezafibrate at t=0 hours versus other experimental conditions, $^{\dagger}p<0.05$ for patient fibroblasts treated with 400 µM bezafibrate at t=0 hours versus other experimental conditions.

3.6. Bezafibrate treatment depletes glutathione during stress

Baseline measurements indicated that bezafibrate treatment affected GSH and mitochondrial metabolism in the VLCAD deficient fibroblasts. As shown above, applying heat stress to these cells caused a significant increase in mitochondrial superoxide levels. To investigate the effect of heat stress on the ability of bezafibrate treated VLCAD deficient cells to maintain GSH levels, we doubled the heat stress duration to 96 hours (Fig. 7).

Control cells pretreated with 0 µM or 400 µM bezafibrate could maintain GSH levels throughout the 96 hour course of heat stress, despite the approximate doubling of mitochondrial superoxide levels that were measured in control cells after 48-hours of heat stress (Fig. 6 & 7). The untreated patient fibroblasts were also able to maintain similar GSH levels during the 96 hours of heat stress (Fig. 7). The bezafibrate treated patient cells, which had significantly higher superoxide levels than the untreated patient cells, experienced an eventual depletion of GSH levels after 96 hours of heat stress (Fig. 7). After 96 hours of heat stress, there was a significant difference in GSH levels in patient fibroblasts pretreated with 0µM versus 400 µM bezafibrate (p=0.032).

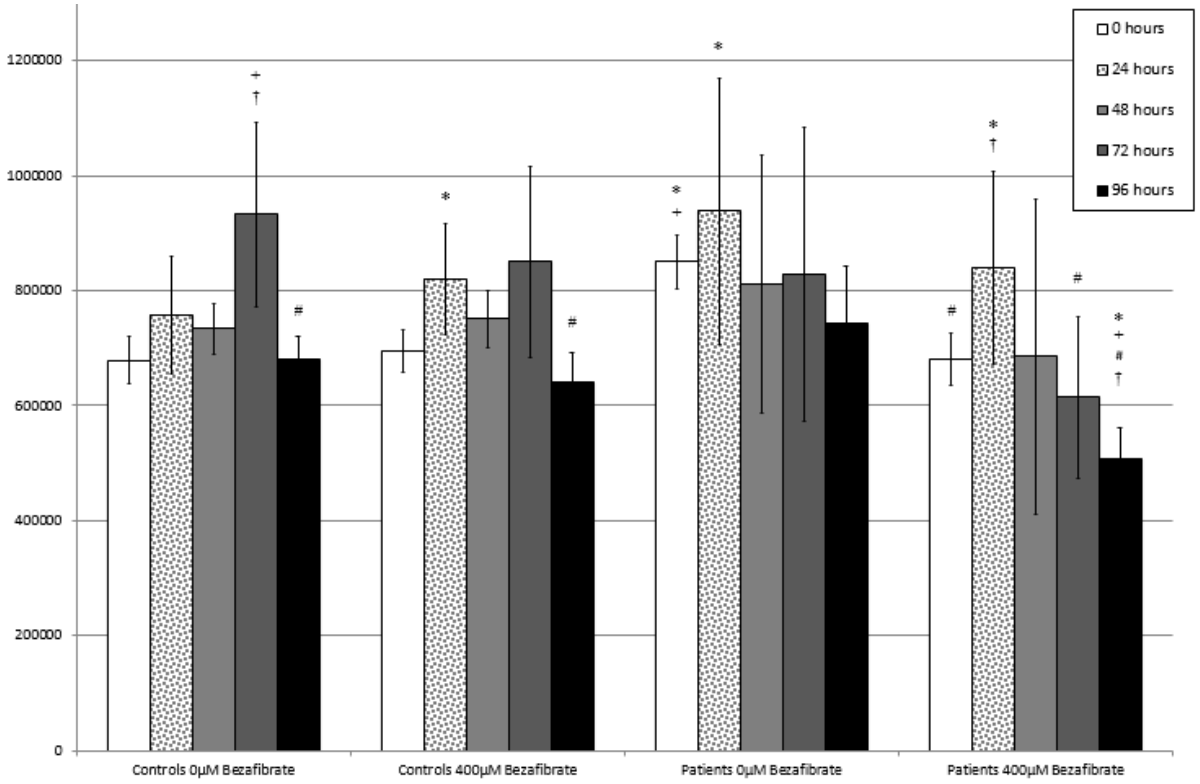

Fig. 7. GSH probe intensity during heat stress

The graph shows reduced GSH (VitaBright43) probe mean intensity (a.u.) for six control or VLCAD deficient dermal fibroblasts cell lines. These were treated either with 0 µM or 400 µM bezafibrate for 96 hours. The pretreated cell lines were subsequently exposed to heat stress (41°C) for 0 hours (solid white), 24 hours (sprinkle pattern), 48 hours (solid light grey), 72 hours (solid dark grey) or 96 hours (solid black). Error bars represent SEM, data from 3(+) independent cultures. Test of statistical significance is presented for the four experimental variables at baseline (heat stress = 0 hours), compared to remaining experimental conditions. Significant p-values (p<0.05) are indicated as: *p<0.05 for control fibroblasts treated with 0 µM bezafibrate at t=0 hours versus other experimental conditions, $^{+}$p<0.05 for control fibroblasts treated with 400 µM bezafibrate at t=0 hours versus remaining experimental conditions, $^{\#}$p<0.05 for patient fibroblasts treated with 0 µM bezafibrate at t=0 hours versus other experimental conditions, †p<0.05 for patient fibroblasts treated with 400 µM bezafibrate at t=0 hours versus other experimental conditions.

3.7. The effects of bezafibrate on total thiols and viability during heat stress

To investigate whether there is a global cellular loss of reduced thiols or if the depletion is specific to GSH we used the total thiol probe (VitaBright48) to measure the total reduced thiol levels over the course of 120 hours of heat stress (Fig. 8). The additional 24 hours were added to the experimental setup to evaluate the effects of the observed GSH depletion after 96 hours of heat stress. Control fibroblasts under both treatment conditions experienced an increase in detectable levels of total reduced thiols as a result of heat stress (Fig. 8). Untreated patient cells also experienced an increase of total reduced thiols as the duration of heat stress increased (Fig. 8). In contrast, the patient cells pretreated with 400 μM bezafibrate did not experience this increase, which can probably be explained by the severe GSH depletion after the 96 hour heat stress time-point in Fig. 7, as GSH represents a large fraction of cellular thiols [61]. Since GSH depletion is an early marker of apoptosis [61], we assayed cellular viability over the 120 hour span of heat stress (Fig. 9). Fasting heat stress resulted in a gradual decrease in viability over time. At the 120 hour time point, there was a significant difference in the percentage of viable cells in patient fibroblasts pretreated with 0 μM versus 400 μM bezafibrate ($p=0.0439$).

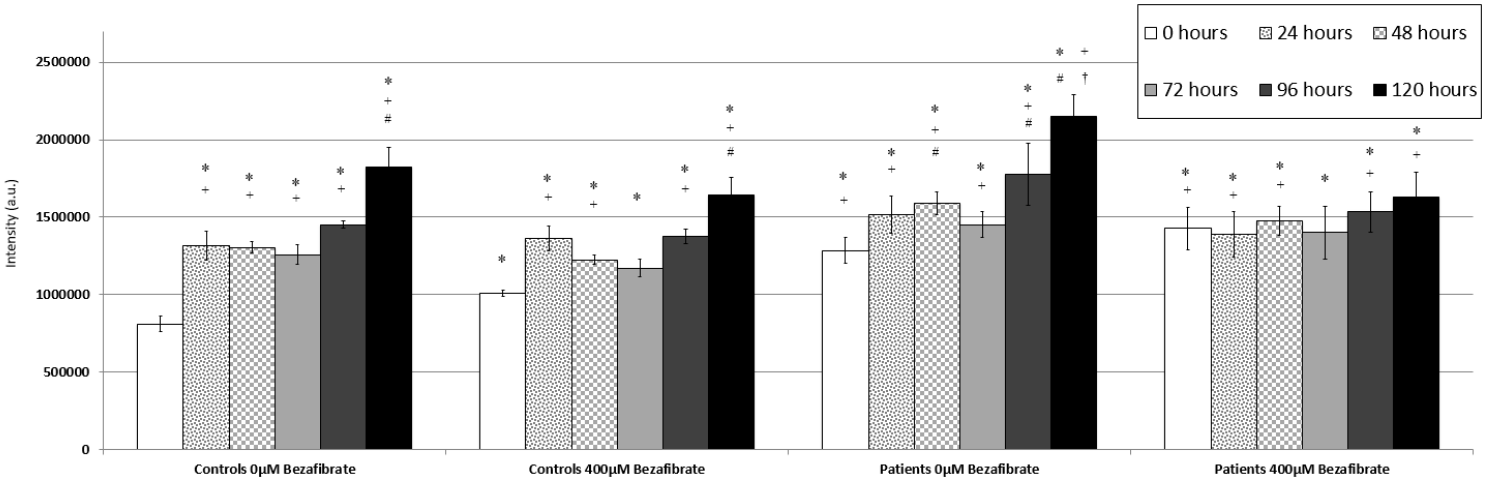

Fig. 8. Total thiol probe during heat stress

The graphs shows total thiols (VitaBright48) probe mean intensity (a.u.) for six control or VLCAD deficient dermal fibroblasts cell lines. These were treated either with 0 µM or 400 µM bezafibrate for 96 hours. The pretreated cell lines were subsequently exposed to heat stress (41°C) for 0 hours (solid white), 24 hours (sprinkle pattern), 48 hours (checkered pattern), 72 hours (solid light grey), 96 hours (solid dark grey) or 120 hours (solid black). Error bars represent SEM, data from 3(+) independent cultures. Test of statistical significance is presented for the four experimental variables at baseline (heat stress = 0 hours), compared to remaining experimental conditions. Significant p-values ($p<0.05$) are indicated as: $^{*}p<0.05$ for control fibroblasts treated with 0 µM bezafibrate at t=0 hours versus other experimental conditions, $^{+}p<0.05$ for control fibroblasts treated with 400 µM bezafibrate at t=0 hours versus remaining experimental conditions, $^{\#}p<0.05$ for patient fibroblasts treated with 0 µM bezafibrate at t=0 hours versus other experimental conditions, $^{\dagger}p<0.05$ for patient fibroblasts treated with 400 µM bezafibrate at t=0 hours versus other experimental conditions.

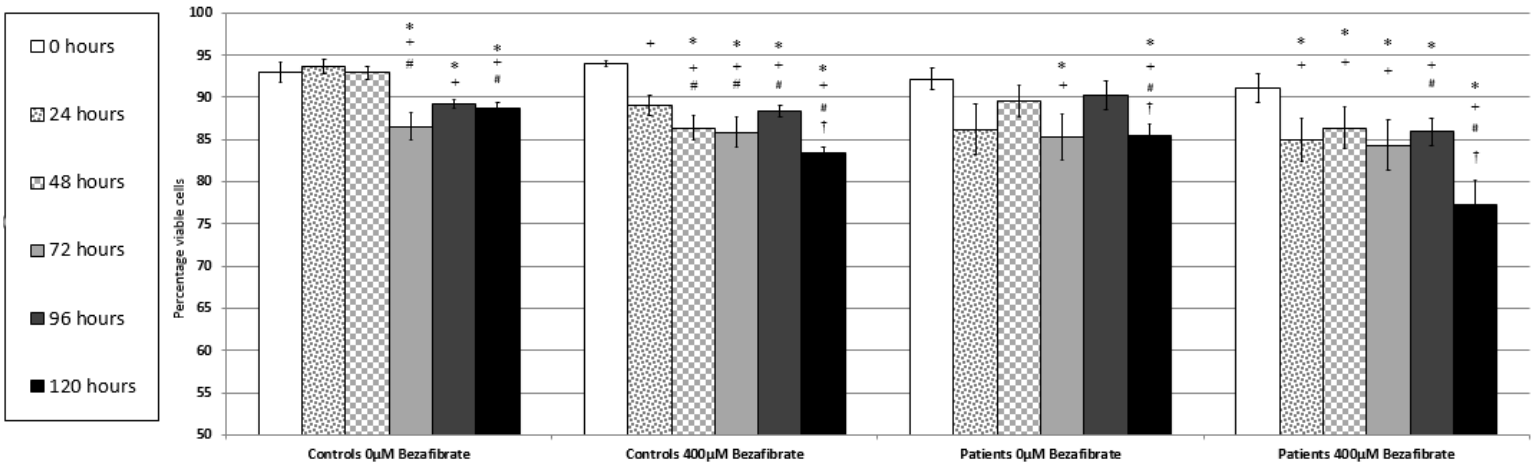

Fig. 9. Cellular viability during heat stress

The graphs shows percentage cellular viability for six control or VLCAD deficient dermal fibroblasts cell lines. These were treated either with 0 µM or 400 µM bezafibrate for 96 hours. The pretreated cell lines were subsequently exposed to heat stress (41°C) for 0 hours (solid white), 24 hours (sprinkle pattern), 48 hours (checkered pattern), 72 hours (solid light grey), 96 hours (solid dark grey) or 120 hours (solid black). Error bars represent SEM, data from 3(+) independent cultures. Test of statistical significance is presented for the four experimental variables at baseline (heat stress = 0 hours), compared to remaining experimental conditions. Significant p-values ($p<0.05$) are indicated as: $^{*}p<0.05$ for control fibroblasts treated with 0 µM bezafibrate at t=0 hours versus other experimental conditions, $^{+}p<0.05$ for control fibroblasts treated with 400 µM bezafibrate at t=0 hours versus remaining experimental conditions, $^{\#}p<0.05$ for patient fibroblasts treated with 0 µM bezafibrate at t=0 hours versus other experimental conditions, $^{\dagger}p<0.05$ for patient fibroblasts treated with 400 µM bezafibrate at t=0 hours versus other experimental conditions.

4. Discussion

In this work we found bioenergetic and redox metabolism in VLCAD deficient cells to be perturbed. Regardless of mutation type, VLCAD deficient patient fibroblasts expressed an increased oxidative stress burden and deranged mitochondrial OXPHOS capacity. Pan-PPAR stimulation with bezafibrate normalized some bioenergetic parameters and did not resolve redox parameters. Applying stress to PPAR stimulated VLCAD deficient cells led to increased redox stress and increased cell death. Our findings further implicate disruption of redox homeostasis with a deranged thiol metabolism as key factors in the long-term pathogenic consequences of chronic PPAR over-activation in VLCAD deficiency.

Deranged mitochondrial OXPHOS capacity in VLCAD deficient cells was evidenced by their decreased CS activity combined with increased activities of respiratory chain complexes I and II/III (Fig. 4). Decreased CS activity might reflect a metabolic shift, where VLCAD deficient cells tend to favor anaerobic glycolysis or entry of glucose into the pentose phosphate pathway. The former is indirectly supported by elevated serum lactic acid levels in VLCAD deficient patients during stress and the latter by the need for maintaining cytosolic NADPH levels to power the GSH antioxidant system due to an increased oxidative burden [2, 67-69]. To some extent, increased respiratory chain activity must also reflect the presence of glutamine in the culture media, which can enter the Krebs cycle independently of CS (as α-ketoglutarate) and thereby help to support sufficient NADPH levels and substrate precursors for GSH maintenance.

Potent PPAR signaling activation via bezafibrate or accumulation of intracellular long-chain fatty acids may force a metabolic shift, away from a previous metabolic adaptation aimed at supporting the higher NADPH consumption associated with increased recycling of GSSH to GSH. This is supported by the bezafibrate induced alterations of metabolic conditions at baseline (Fig. 4A-C), and the decreased GSH levels (Fig. 5A) without a concurrent decrease in mitochondrial superoxide levels (Fig. 3). This would also explain why fasting heat stress has more severe consequences for the bezafibrate treated patient cells as discussed below.

Several works have previously found an increased oxidative burden in cells and animals with VLCAD deficiency [16, 19, 20]. The cause is probably a combination of increased ROS production and decreased capacity for removing ROS and repairing oxidation products.

Several components of mitochondrial respiratory chain are major contributors to the total cellular production of ROS and the integrity of the flow of electrons through the respiratory chain is vital for minimizing the production of ROS [63, 70-72]. VLCAD deficiency can lead to elevated superoxide production as a result of increased electron leakage from the respiratory chain in multiple ways. VLCAD deficiency is characterized by a deceased FAO flux and accumulation of non-oxidizable lipid species, especially long-chain acyl-CoAs and acyl-carnitines. Because of the lipophilic nature of these lipids, some will accumulate in the inner mitochondrial membrane, thereby disturbing the cristae structure, which is a prerequisite for proper function of the mitochondrial respiratory chain, which in turn will increase electron leakage and superoxide production [18, 72]. In addition, normal VLCAD protein has a close physical association with the mitochondrial respiratory chain and may well serve a moonlighting function as a chaperone that serves to stabilize the respiratory chain supercomplexes. Hence, absent or altered VLCAD protein might destabilize the respiratory chain supercomplexes, in a similar manner to what has been reported for a structurally similar VLCAD isoform (ACAD9) [73-75]. Finally, PPAR activation leads to increased biogenesis of multiple mitochondrial components, including those responsible for mitochondrial ROS production. If this biogenesis is not balanced, it will cause cellular dysfunction [39, 76, 77]. There is some evidence that patients with long-chain FAO disorders suffer from chronic overactivation of PPAR, which is consistent with the fact that these patients accumulate long-chain fatty acids with the associated acyl-CoAs and acyl-carnitines, as these metabolites are the primary endogenous PPAR agonists in terms of binding potency and quantity [39, 40, 78]. Culturing long-chain FAO disorder patient cells in media supplemented with long-chain fatty acids does lead to chronic PPAR overactivation [39]. Likewise, exposing VLCAD deficient mice to fasting and resultant lipid recruitment leads to extensive proteomic changes of which bioinformatical analysis reveal PPARα activation to be a crucial signaling pathway [79]. It is therefore possible that PPAR overactivation drives excessive accumulation of some

mitochondrial components, such as respiratory chain complex I, which coupled with increased rate of electron leakage from these redox proteins is the causative factor for increased superoxide production observed in this and other studies.

Increased superoxide production in turn can damage components of the mitochondrial respiratory chain via oxidation, initiating a vicious circle, with the result that some VLCAD patients develop secondary respiratory deficiencies, as indeed we also find in this study. The vicious circle can continue further, for example resulting in vitamin or cofactor deficiencies. Electron donation to respiratory chain complex III from β-oxidation via electron-transfer flavoprotein and electron-transfer flavoprotein dehydrogenase is dependent on the inner mitochondrial membrane CoQ10 pool, as is electron donation from mitochondrial respiratory complex I and complex II. Levels of CoQ10 in muscle tissue of some VLCAD deficient patients have been found to be reduced [15]. Endosynthesis capacity of CoQ10 has also been found to be lower in VLCAD deficient cells, compared to controls [80]. An increased oxidative burden coupled with reduced CoQ10 endosynthesis may lead to development of secondary CoQ10 deficiency, leading to a respiratory chain electron flow blockage and thereby further increasing superoxide levels [2, 15, 80]. Because VLCAD deficient patients consume a modified diet, decreased dietary intake of CoQ10 may increase the risk of developing secondary CoQ10 deficiency [81]. Because of their dysfunctional mitochondria and abnormal responses to bezafibrate treatment, we were interested in studying the pathogenic consequences of exposing VLCAD deficient cells to bezafibrate in combination with a relevant stress factor, such as fasting heat stress. We found that the combined treatment depletes the essential thiol antioxidant GSH concurrent with a significant increase of mitochondrial ROS and reduction of cellular viability (Fig. 6-8).

Thiols are already known to be implicated in long-chain FAO disorders, due to the requirement for activation of fatty acids by attachment of a CoA by a thioester link prior to import into the mitochondria by the carnitine shuttle and again for subsequent β-oxidation in the matrix [7]. Experimental data and *in silico* modeling have already indicated that intracellular accumulation and excretion of acyl-CoAs can result in a sequestration of CoA, which can produce a potent

non-length specific inhibition of β-oxidation and other essential cellular functions [22, 66]. When this occurs, the result is a dramatic reduction of overall FAO flux. This is clinically relevant, for instance, in cases of hypoketotic hypoglycemia in well managed patients and in nonresponders to medium-chain fatty acid supplementation, as well as in other situations where CoA and carnitine sequestration could explain the inability to maintain energy homeostasis, despite the availability of bioenergetic substrates that bypass VLCAD deficiency [22, 65, 66]. Circulating acyl-CoAs can also provide a long-term lipotoxic effect, for example, by activating NADPH oxidases and thus increasing ROS levels in various muscle tissues [82]. Additionally, oxidative and metabolic stress can result in widespread protective posttranslational protein modification with CoA [83]. As both stressors are present in long-chain FAO disorders, this can result in further sequestration of CoA.

Although we did not measure CoA levels in the present study, a challenged GSH metabolism may contribute to dysregulated CoA metabolism in long-chain FAO disorders. Chronically elevated consumption of GSH provides a demand on the cellular thiol/cysteine pool, and this demand increases at times of metabolic crisis. Free cysteine is cytotoxic and therefore cannot be allowed to accumulate as a free amino acid, hence the availability of cysteine at any one time is limited [84]. The relative cellular priority given to phosphopantothenoylcysteine synthetase (CoA synthesis) and glutamate-cysteine ligase (GSH synthesis) during various physiological conditions is not well-described. But as cellular cysteine levels decrease, glutamate-cysteine ligase activity is increased by posttranslational modification, thus maintaining GSH production. The result is that GSH synthesis takes up increasingly larger fractions of the available cysteine pool as cysteine levels drop [84]. Since GSH is the most abundant non-protein thiol-containing compound, its synthesis probably consumes an appreciable part of the cellular cysteine production, especially in cells/tissues with pathologically high levels of oxidative stress as seen in VLCAD deficiency. Acute oxidative stress can further increase this overconsumption. For example, during oxidative bursts protective posttranslational addition of GSH (glutathionylation) can increase an order of magnitude, thus providing a further thiol/cysteine sink. Another example is oxidized GSSG. If insufficient NADPH is available to power recycling of GSSG to GSH, GSSG is exported into the circulatory system and

thus represents an acute intracellular thiol loss [85]. Maintenance of GSH levels by NADPH dependent recycling and de-novo synthesis is energetically demanding, further burdening the already overworked and dysfunctional cellular bioenergetic system in VLCAD deficient cells [23, 86, 87]. During episodes of increased stress and resultant ROS production, the increased energy demand leads to fatty acid recruitment, which in VLCAD deficient cells results in sequestration of CoA in the form of acyl-CoA [44]. This means that during stress, two strong demands are placed on the cellular thiol/cysteine pool. On the one hand, GSH synthesis can win out, potentially leading to decreased CoA levels and deceased FAO flux, which will result in lipotoxicity and in the end will affect mitochondrial NADPH levels and thus antioxidant function [23]. Alternatively, GSH can become depleted, leading to oxidative damage. Depletion of GSH levels will allow a vicious cycle of oxidative damage leading to even higher ROS levels, due to an inability to repair oxidative damage to cellular structures coordinating redox biochemistry and a resulting greater leakage of electrons from these [63, 88-90]. This leads to further oxidative damage, which itself can harm mitochondrial and cellular function. For instance, severe/acute GSH depletion can prevent mitochondrial ATP synthesis by allowing oxidative modifications to shut down the inner membrane ATP/ADP translocator, likewise cellular bioenergetic function in VLCAD deficient cells has be found to be improved by mitochondrial targeted antioxidants [16, 91]. PPAR overactivation has previously been related to thiol metabolism, for example exposing normal Wistar rats to a pan-PPAR agonist (with a high affinity towards PPARα) causes changes in plasma and urine levels of cysteine, homocysteine, and B-vitamins related to thiol metabolism [92].

A relatively slow degradation of mitochondrial quality and function driven by oxidative stress and associated pathological factors could be a primary causative factor for the late onset of myopathic symptoms in VLCAD deficient patients. Severe oxidative damage has been shown to be the primary etiological factor in some inborn early-onset myopathies supporting the notion that skeletal muscle under some circumstances may be especially vulnerable to redox disturbances [93]. With regard to GSH and development of myopathic symptoms, inhibition of GSH synthesis was required in order to induce rhabdomyolysis in a fibrate and/or statin treated mice model, linking PPAR overactivation, acute GSH depletion and rhabdomyolysis [94]. Fig. 10

shows a schematic representation of how different stressors involved in long-chain FAO deficiency can interact and enhance one another in a vicious feed-forward cycle.

Removal of bezafibrate in the circulation is quite rapid, whereas the lack of relevant enzymes in cell culture means that the half-time of bezafibrate in culture media in all likelihood is greater [95]. This also means that the effects of bezafibrate in this study do not completely match the *in vivo* effects, as indeed cell culture never does. However, it does support the notion that chronic overactivation of PPARs is cytotoxic and especially so in long-chain FAO disorders. This is supported by the well-described *in vivo* toxicity profile of the different fibrates. Whereas the *in vivo* mitochondrial and muscle toxicity of rapidly metabolized fibrates like bezafibrate is low, it is much higher for the slowly metabolized fibrates or fibrates with active metabolites [96-98].

In our experimental setup, the presence of lipids in the culture media is very limited. This means that our experimental setup can be thought of as providing evidence of the deleterious effects of PPAR activation alone, relatively isolated from other lipotoxic factors, such as membrane distortion.

5. Conclusion

In this work, we found that mitochondrial metabolic capacity and the essential peptide GSH is affected by bezafibrate treatment of VLCAD deficient fibroblasts, even at basal conditions. Further, we found that cellular GSH levels and viability can be reduced following a bezafibrate/PPAR driven increase in mitochondrial ROS levels during exposure to fasting heat stress. The bezafibrate/PPAR driven depletion of GSH, in VLCAD deficient cells, adds a new aspect to the role of thiol metabolism in VLCAD deficiency. As the density of damaged mitochondrial structures increases, the repair/mitophagy system can become overwhelmed, leading to further disruption of cellular function and release of proinflammatory mitochondrial structures into the local extracellular environment, further amplifying the vicious cycle [99]. Such mechanisms may be involved in the disabling attacks of rhabdomyolysis that characterize the myopathic forms of VLCAD deficiency. Therefore, it is of interest to further study GSH, CoA and overall thiol metabolism in patients with long-chain FAO disorders and if present findings translate well to patients, it will be of interest to find therapeutic approaches for supporting mitochondrial function by protecting cells against GSH and thiol depletion in long-chain FAO disorders. It would be possible to treat insufficient cysteine levels by dietary supplementation [100], by supplying cell and organelle permeable reduced GSH-esters or mitochondria targeting antioxidant compounds during acute crises [16, 101, 102], by increasing the activity of the rate-limiting step of GSH synthesis [103, 104] and by supporting NADPH homeostasis.

While the interest within the field of long-chain FAO disorders has shifted towards more specific PPAR subtype activators than bezafibrate, it is quite likely that halting long-term disease progression could benefit from some degree of periodic PPAR(α) suppression, as has been previously proposed [39]. The role of PPAR activation and PPARα overactivation within the long-chain FAO disorder warrant further study, as it has a high potential for improving our understanding of the pathogenic process, which can lead to the development of improved treatment options.

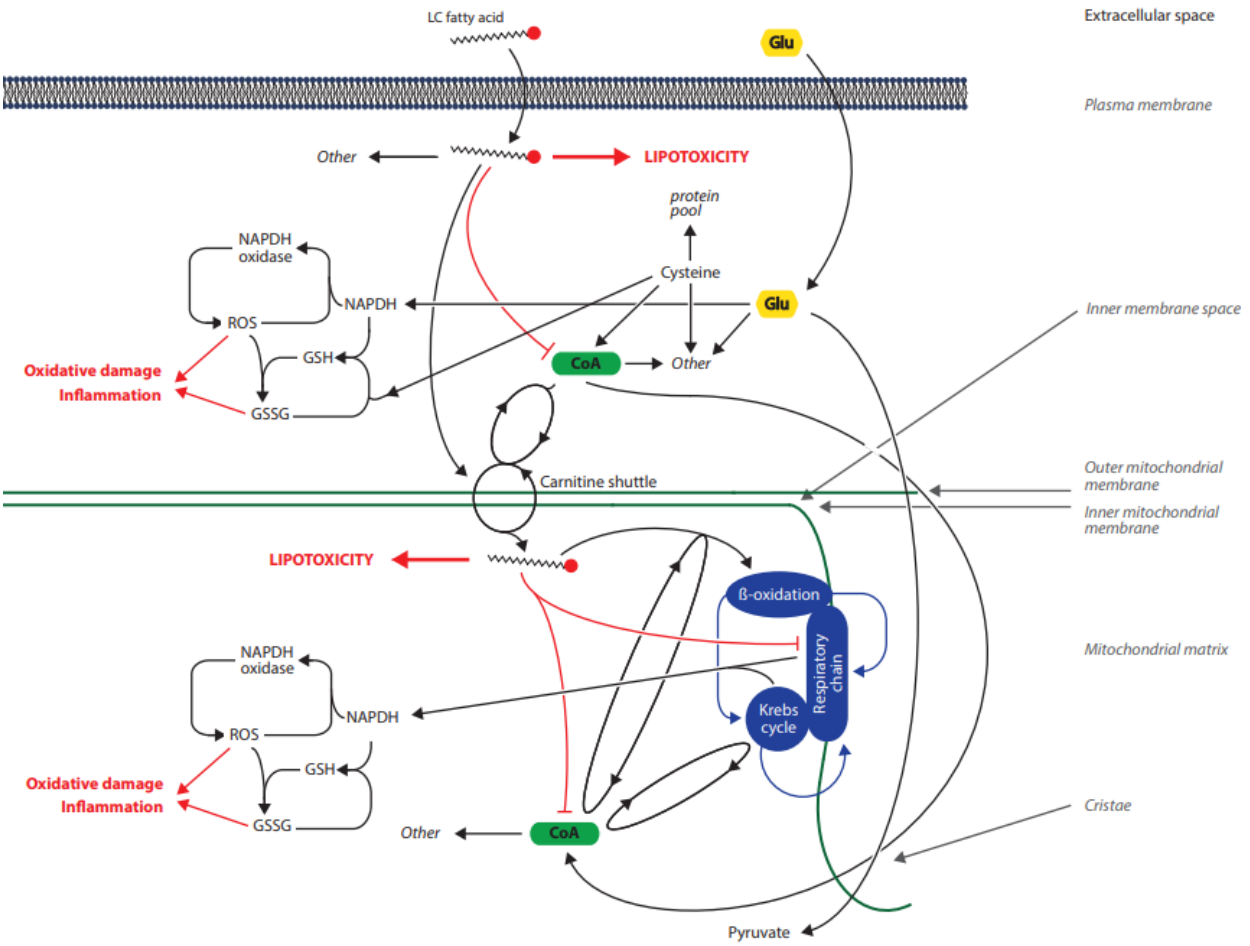

Fig. 10. Stress pathways in VLCAD deficiency

Schematic representation of how some of the different stressors involved in long-chain FAO deficiency can interact and enhance one another in a vicious feed-forward cycle. These stressors include:

1: lipotoxicity (including PPAR(α) overactivation, CoA sequestration and disruption of cellular membranes)

2: deranged or insufficient thiol metabolism

3: increased ROS generation

4: secondarily deficient OXPHOS system components

5: inflammation

Illustration: courtesy of Dorte Tranbjerg Hansen

Acknowledgments

Aarhus University Research Unit for Molecular Medicine wishes to thank their colleagues and patient collaborators all over the world. Martin Lund wishes to express his gratitude to Ultragenyx Pharmaceutical Inc. and Aarhus University Faculty of Health Graduate School for funding and to Dr. Iain Hargreaves and Robert Heaton for their great hospitality while hosting him in Liverpool, England.

Supplementary data

Control	Abbreviation	Vendor	Lot identifier
Control 1	**C1**	Cambrex	CC-2509/5F0438
Control 2	**C2**	ATCC	CRL-2450
Control 3	**C3**	PromoCell	0083002.2
Control 4	**C4**	PromoCell	1032107.2
Control 5	**C5**	PromoCell	9052801.2
Control 6	**C6**	PromoCell	9060902.2

Supplementary Table 1.

Commercial human dermal fibroblasts control cell lines vendor information

.

Supplementary figures

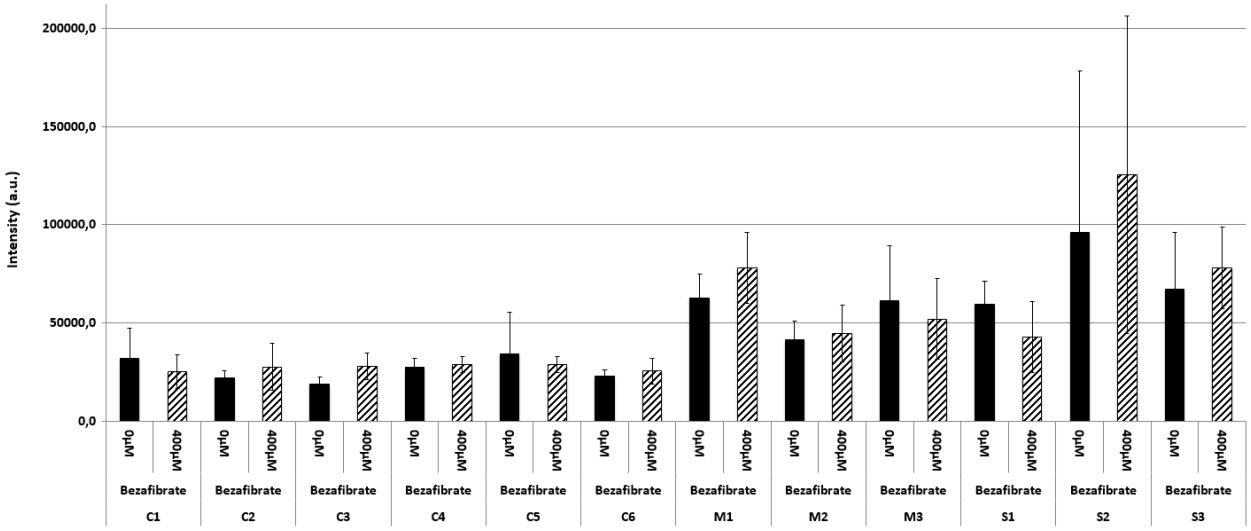

Fig. S.1A. Individual cell line MitoSox probe intensity

Graph shows MitoSox probe mean intensity (a.u.) for six individual control or VLCAD deficient dermal fibroblasts cell lines. These were treated either with 0 µM (solid bars) or 400 µM (dashed bars) bezafibrate for 96 hours. Error bars represent SD, data from 3(+) independent cultures. Controls 1-6 are abbreviated as C1-C6. Mild phenotype patients 1-3 are abbreviated as M1-3. Severe phenotype patients 1-3 are abbreviated as S1-3.

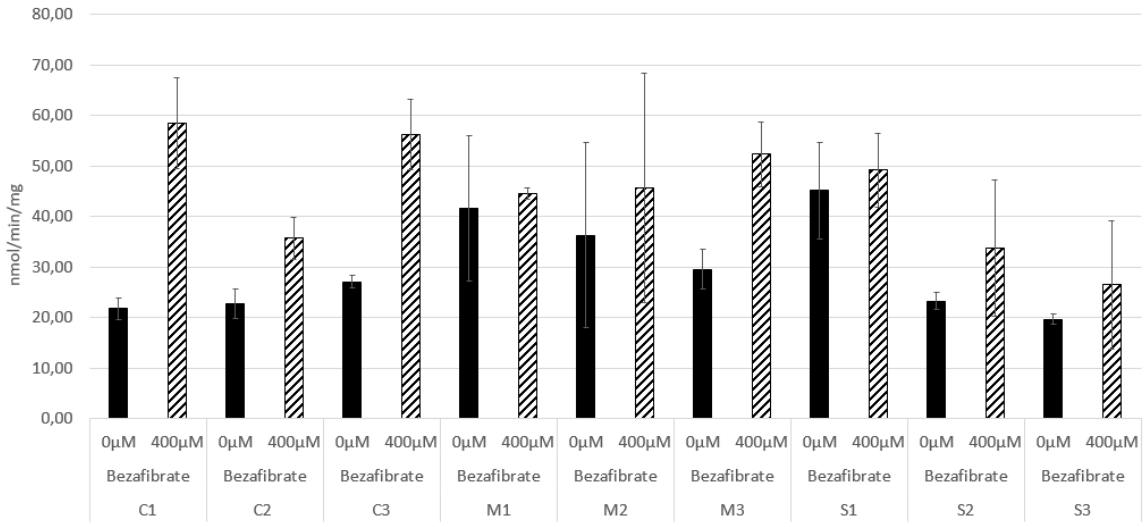

Fig S.1B. Individual cell line complex I activity

Graph shows respiratory chain complex I mean maximum activity ((nmol/min)/mg protein) for three individual control and six VLCAD deficient dermal fibroblasts cell lines. These were treated either with 0 µM (solid bars) or 400 µM (dashed bars) bezafibrate for 96 hours. Error bars represent SD, data from 2(+) independent cultures. Controls 1-6 are abbreviated as C1-C6. Mild phenotype patients 1-3 are abbreviated as M1-3. Severe phenotype patients 1-3 are abbreviated as S1-3.

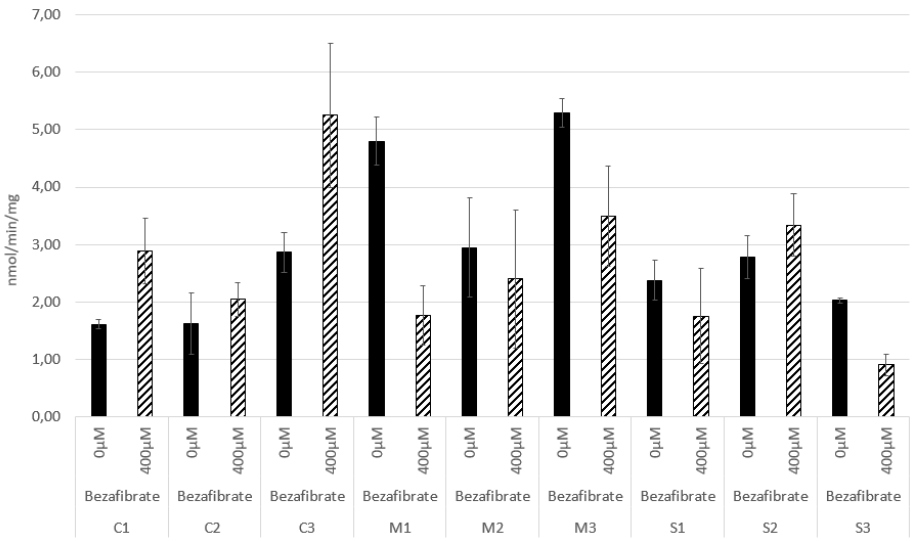

Fig. S.1C. Individual cell line complex II/III activity

Graph shows respiratory chain complex II/III mean maximum activity ((nmol/min)/mg protein) for three individual control and six VLCAD deficient dermal fibroblasts cell lines. These were treated either with 0 µM (solid bars) or 400 µM (dashed bars) bezafibrate for 96 hours. Error bars represent SD, data from 2(+) independent cultures. Controls 1-6 are abbreviated as C1-C6. Mild phenotype patients 1-3 are abbreviated as M1-3. Severe phenotype patients 1-3 are abbreviated as S1-3.

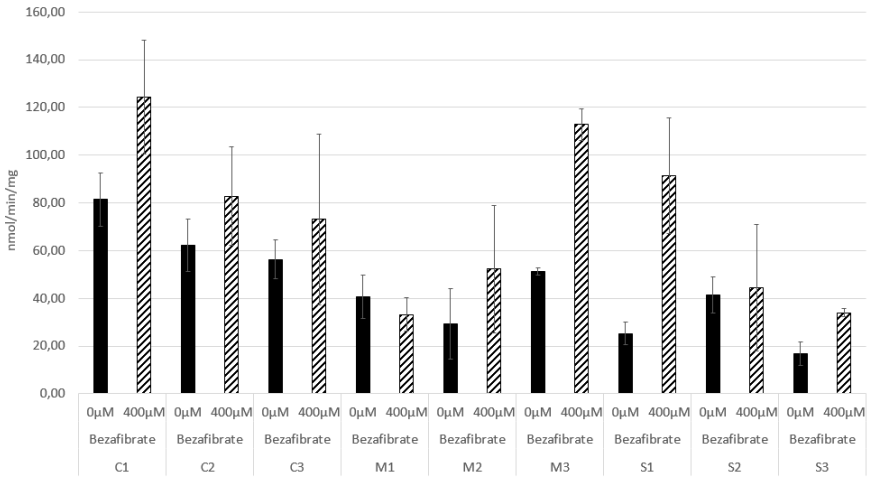

Fig. S.1D. Individual cell line citrate synthase activity

Graph shows Krebs cycle enzyme citrate synthase mean maximum activity ((nmol/min)/mg protein) for three individual control and six VLCAD deficient dermal fibroblasts cell lines. These were treated either with 0 µM (solid bars) or 400 µM (dashed bars) bezafibrate for 96 hours. Error bars represent SD, data from 2(+) independent cultures. Controls 1-6 are abbreviated as C1-C6. Mild phenotype patients 1-3 are abbreviated as M1-3. Severe phenotype patients 1-3 are abbreviated as S1-3.

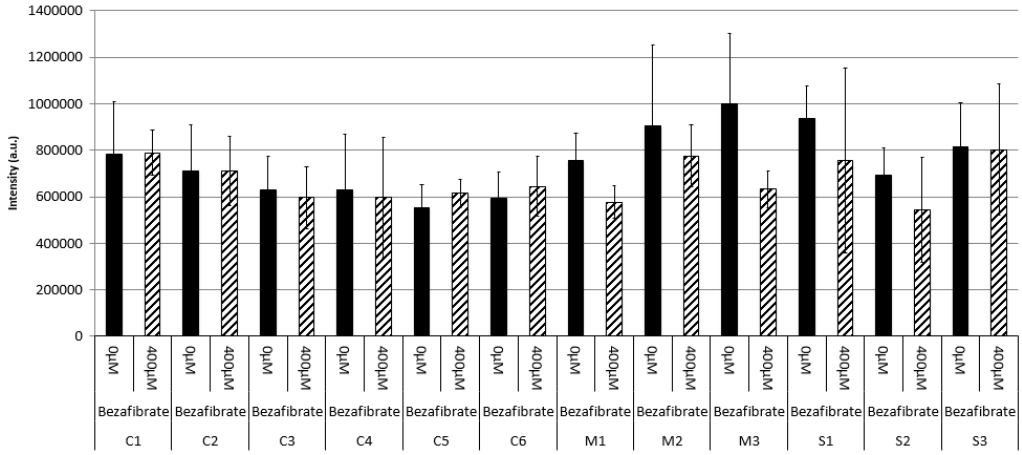

Fig. S.1E. Individual cell line GSH probe intensity

Graph shows reduced GSH (VitaBright43) probe mean intensity (a.u.) for six individual control or VLCAD deficient dermal fibroblasts cell lines. These were treated either with 0 μM (solid bars) or 400 μM (dashed bars) bezafibrate for 96 hours. Error bars represent SD, data from 3(+) independent cultures. Controls 1-6 are abbreviated as C1-C6. Mild phenotype patients 1-3 are abbreviated as M1-3. Severe phenotype patients 1-3 are abbreviated as S1-3.

References

[1] C. Bertrand, C. Largilliere, M.T. Zabot, M. Mathieu, C. Vianeysaban, Very Long-Chain Acyl-CoA Dehydrogenase-Deficiency - Identification of a New Inborn Error of Mitochondrial Fatty-Acid Oxidation in Fibroblasts, Biochimica Et Biophysica Acta 1180(3) (1993) 327-329.
[2] B. Wilcken, Fatty acid oxidation disorders: outcome and long-term prognosis, Journal of Inherited Metabolic Disease 33(5) (2010) 501-506.
[3] R.P. McAndrew, Y. Wang, A.-W. Mohsen, M. He, J. Vockley, J.-J.P. Kim, Structural Basis for Substrate Fatty Acyl Chain Specificity: crystal structure of human very long-chain acyl-CoA dehydrogenase, Journal of Biological Chemistry 283(14) (2008) 9435-9443.
[4] A.J. Bakermans, M.S. Dodd, K. Nicolay, J.J. Prompers, D.J. Tyler, S.M. Houten, Myocardial energy shortage and unmet anaplerotic needs in the fasted long-chain acyl-CoA dehydrogenase knockout mouse, Cardiovascular Research 100(3) (2013) 441-449.
[5] J. Ritterhoff, R. Tian, Metabolism in cardiomyopathy: every substrate matters, Cardiovascular Research 113(4) (2017) 411-421.
[6] S.M. Houten, S. Violante, F.V. Ventura, R.J.A. Wanders, The Biochemistry and Physiology of Mitochondrial Fatty Acid β-Oxidation and Its Genetic Disorders, Annual Review of Physiology 78(1) (2016) 23-44.
[7] S.M. Houten, R.J. Wanders, A general introduction to the biochemistry of mitochondrial fatty acid beta-oxidation, J Inherit Metab Dis 33(5) (2010) 469-77.
[8] S.J.G. Knottnerus, J.C. Bleeker, R.C.I. Wüst, S. Ferdinandusse, L. Ijlst, F.A. Wijburg, R.J.A. Wanders, G. Visser, R.H. Houtkooper, Disorders of mitochondrial long-chain fatty acid oxidation and the carnitine shuttle, Reviews in Endocrine and Metabolic Disorders (2018).
[9] B.S. Andresen, S. Olpin, B.J.H.M. Poorthuis, H.R. Scholte, C. Vianey-Saban, R. Wanders, L. Ijlst, A. Morris, M. Pourfarzam, K. Bartlett, E.R. Baumgartner, J.B.C. deKlerk, L.D. Schroeder, T.J. Corydon, H. Lund, V. Winter, P. Bross, L. Bolund, N. Gregersen, Clear Correlation of Genotype with Disease Phenotype in Very–Long-Chain Acyl-CoA Dehydrogenase Deficiency, The American Journal of Human Genetics 64(2) (1999) 479-494.
[10] S.M. Houten, H. Herrema, H. te Brinke, S. Denis, J.P.N. Ruiter, T.H. van Dijk, C.A. Argmann, R. Ottenhoff, M. Müller, A.K. Groen, F. Kuipers, D.-J. Reijngoud, R.J.A. Wanders, Impaired amino acid metabolism contributes to fasting-induced hypoglycemia in fatty acid oxidation defects, Human Molecular Genetics 22(25) (2013) 5249-5261.
[11] H. Li, S. Fukuda, Y. Hasegawa, J. Purevsuren, H. Kobayashi, Y. Mushimoto, S. Yamaguchi, Heat stress deteriorates mitochondrial β-oxidation of long-chain fatty acids in cultured fibroblasts with fatty acid β-oxidation disorders, Journal of Chromatography B 878(20) (2010) 1669-1672.
[12] B.A. van Adel, M.A. Tarnopolsky, Metabolic Myopathies: Update 2009, Journal of Clinical Neuromuscular Disease 10(3) (2009) 97-121.
[13] S. Tucci, D. Herebian, M. Sturm, A. Seibt, U. Spiekerkoetter, Tissue-specific strategies of the very-long chain acyl-CoA dehydrogenase-deficient (VLCAD-/-) mouse to compensate a defective fatty acid β-oxidation, PloS one 7(9) (2012) e45429-e45429.
[14] E.F. Diekman, G. Visser, J.P.J. Schmitz, R.A.J. Nievelstein, M. de Sain-van der Velden, M. Wardrop, W.L. Van der Pol, S.M. Houten, N.A.W. van Riel, T. Takken, J.A.L. Jeneson, Altered Energetics of Exercise Explain Risk of Rhabdomyolysis in Very Long-Chain Acyl-CoA Dehydrogenase Deficiency, PLOS ONE 11(2) (2016) e0147818.
[15] P. Laforet, C. Acquaviva-Bourdain, O. Rigal, M. Brivet, I. Penisson-Besnier, B. Chabrol, D. Chaigne, O. Boespflug-Tanguy, C. Laroche, A.L. Bedat-Millet, A. Behin, I. Delevaux, A. Lombes, B.S. Andresen, B. Eymard, C. Vianey-Saban, Diagnostic assessment and long-term follow-up of 13 patients with Very Long-Chain Acyl-Coenzyme A dehydrogenase (VLCAD) deficiency, Neuromuscul Disord 19(5) (2009) 324-9.

[16] B. Seminotti, G. Leipnitz, A. Karunanidhi, C. Kochersperger, V.Y. Roginskaya, S. Basu, Y. Wang, P. Wipf, B. Van Houten, A.-W. Mohsen, J. Vockley, Mitochondrial energetics is impaired in very long-chain acyl-CoA dehydrogenase deficiency and can be rescued by treatment with mitochondria-targeted electron scavengers, Human molecular genetics 28(6) (2018) 928-941.
[17] M. Lund, R.K.J. Olsen, N. Gregersen, A short introduction to acyl-CoA dehydrogenases; deficiencies and novel treatment strategies, Expert Opinion on Orphan Drugs (2015) 1-12.
[18] M. Wajner, Alexandre U. Amaral, Mitochondrial dysfunction in fatty acid oxidation disorders: insights from human and animal studies, Biosci Rep 36(1) (2016) e00281.
[19] P. Fernandez-Guerra, M. Lund, T.J. Corydon, N. Cornelius, N. Gregersen, J. Palmfeldt, P. Bross, Application of an Image Cytometry Protocol for Cellular and Mitochondrial Phenotyping on Fibroblasts from Patients with Inherited Disorders, Springer Berlin Heidelberg2015, pp. 1-10.
[20] S. Tucci, S. Primassin, U. Spiekerkoetter, Fasting-induced oxidative stress in very long chain acyl-CoA dehydrogenase-deficient mice, FEBS Journal 277(22) (2010) 4699-4708.
[21] R.K. Olsen, N. Cornelius, N. Gregersen, Genetic and cellular modifiers of oxidative stress: what can we learn from fatty acid oxidation defects?, Mol Genet Metab 110 Suppl (2013) S31-9.
[22] K. van Eunen, C.M.L. Volker-Touw, A. Gerding, A. Bleeker, J.C. Wolters, W.J. van Rijt, A.-C.M.F. Martines, K.E. Niezen-Koning, R.M. Heiner, H. Permentier, A.K. Groen, D.-J. Reijngoud, T.G.J. Derks, B.M. Bakker, Living on the edge: substrate competition explains loss of robustness in mitochondrial fatty-acid oxidation disorders, BMC Biology 14(1) (2016) 107.
[23] M. Marí, A. Morales, A. Colell, C. García-Ruiz, N. Kaplowitz, J.C. Fernández-Checa, Mitochondrial glutathione features, regulation and role in disease, Biochimica et biophysica acta 1830(5) (2013) 3317-3328.
[24] F. Djouadi, F. Aubey, D. Schlemmer, J.P.N. Ruiter, R.J.A. Wanders, A.W. Strauss, J. Bastin, Bezafibrate increases very-long-chain acyl-CoA dehydrogenase protein and mRNA expression in deficient fibroblasts and is a potential therapy for fatty acid oxidation disorders, Human Molecular Genetics 14(18) (2005) 2695-2703.
[25] F. Djouadi, J.P. Bonnefont, L. Thuillier, V. Droin, N. Khadom, A. Munnich, J. Bastin, Correction of fatty acid oxidation in carnitine palmitoyl transferase 2-deficient cultured skin fibroblasts by bezafibrate, Pediatric research 54(4) (2003) 446-51.
[26] M.C. Orngreen, K.L. Madsen, N. Preisler, G. Andersen, J. Vissing, P. Laforet, Bezafibrate in skeletal muscle fatty acid oxidation disorders: A randomized clinical trial, Neurology (2014).
[27] J.-P. Bonnefont, J. Bastin, A. Behin, F. Djouadi, Bezafibrate for an Inborn Mitochondrial Beta-Oxidation Defect, New England Journal of Medicine 360(8) (2009) 838-840.
[28] B.J. P, B. J, L. P, A. F, M. A, R. S, R. D, G.-L. S, V. A, B. A, E. B, B.J. L, D. F, Long-Term Follow-Up of Bezafibrate Treatment in Patients With the Myopathic Form of Carnitine Palmitoyltransferase 2 Deficiency, Clinical Pharmacology & Therapeutics 88(1) (2010) 101-108.
[29] M. Ørngreen, J. Vissing, P. Laforét, No effect of bezafibrate in patients with CPTII and VLCAD deficiencies, Journal of Inherited Metabolic Disease 38(2) (2015) 373-374.
[30] J. Bastin, J.-P. Bonnefont, F. Djouadi, J.-L. Bresson, Should the beneficial impact of bezafibrate on fatty acid oxidation disorders be questioned?, Journal of Inherited Metabolic Disease 38(2) (2015) 371-372.
[31] K. Yamada, H. Shiraishi, E. Oki, M. Ishige, T. Fukao, Y. Hamada, N. Sakai, F. Ochi, A. Watanabe, S. Kawakami, K. Kuzume, K. Watanabe, K. Sameshima, K. Nakamagoe, A. Tamaoka, N. Asahina, S. Yokoshiki, T. Miyakoshi, K. Ono, K. Oba, T. Isoe, H. Hayashi, S. Yamaguchi, N. Sato, Open-label clinical trial of bezafibrate treatment in patients with fatty acid oxidation disorders in Japan, Molecular genetics and metabolism reports 15 (2018) 55-63.
[32] J. Berger, D.E. Moller, The mechanisms of action of PPARs, Annu Rev Med 53 (2002) 409-35.

[33] J.C. Komen, D.R. Thorburn, Turn up the power – pharmacological activation of mitochondrial biogenesis in mouse models, British Journal of Pharmacology 171(8) (2014) 1818-1836.
[34] J.-L. Li, Q.-Y. Wang, H.-Y. Luan, Z.-C. Kang, C.-B. Wang, Effects of L-carnitine against oxidative stress in human hepatocytes: involvement of peroxisome proliferator-activated receptor alpha, Journal of Biomedical Science 19(1) (2012) 32.
[35] T. Tanaka, J. Yamamoto, S. Iwasaki, H. Asaba, H. Hamura, Y. Ikeda, M. Watanabe, K. Magoori, R.X. Ioka, K. Tachibana, Y. Watanabe, Y. Uchiyama, K. Sumi, H. Iguchi, S. Ito, T. Doi, T. Hamakubo, M. Naito, J. Auwerx, M. Yanagisawa, T. Kodama, J. Sakai, Activation of peroxisome proliferator-activated receptor δ induces fatty acid β-oxidation in skeletal muscle and attenuates metabolic syndrome, Proceedings of the National Academy of Sciences 100(26) (2003) 15924-15929.
[36] S. Yatsuga, A. Suomalainen, Effect of bezafibrate treatment on late-onset mitochondrial myopathy in mice, Hum Mol Genet 21(3) (2012) 526-35.
[37] H. Lee, Y. Yoon, Mitochondrial fission and fusion, Biochemical Society transactions 44(6) (2016) 1725-1735.
[38] J.M. Suárez-Rivero, M. Villanueva-Paz, P. de la Cruz-Ojeda, M. de la Mata, D. Cotán, M. Oropesa-Ávila, I. de Lavera, M. Álvarez-Córdoba, R. Luzón-Hidalgo, J.A. Sánchez-Alcázar, Mitochondrial Dynamics in Mitochondrial Diseases, Diseases 5(1) (2017) 1.
[39] M. Wakabayashi, Y. Kamijo, T. Nakajima, N. Tanaka, E. Sugiyama, T. Yangyang, T. Kimura, T. Aoyama, Fatty Acid Accumulation and Resulting PPAR Activation in Fibroblasts due to Trifunctional Protein Deficiency, PPAR Research 2012 (2012) 7.
[40] Y. Yang, Y. Feng, X. Zhang, T. Nakajima, N. Tanaka, E. Sugiyama, Y. Kamijo, T. Aoyama, Activation of PPARα by fatty acid accumulation enhances fatty acid degradation and sulfatide synthesis, The Tohoku Journal of Experimental Medicine 240(2) (2016) 113-122.
[41] B. Tandler, C.L. Hoppel, J.A. Mears, Morphological Pathways of Mitochondrial Division, Antioxidants 7(2) (2018) 30.
[42] J. Demers-Lamarche, G. Guillebaud, M. Tlili, K. Todkar, N. Bélanger, M. Grondin, A.P. Nguyen, J. Michel, M. Germain, Loss of Mitochondrial Function Impairs Lysosomes, Journal of Biological Chemistry 291(19) (2016) 10263-10276.
[43] F. Djouadi, F. Habarou, C. Le Bachelier, S. Ferdinandusse, D. Schlemmer, J.F. Benoist, A. Boutron, B.S. Andresen, G. Visser, P. de Lonlay, S. Olpin, T. Fukao, S. Yamaguchi, A.W. Strauss, R.J.A. Wanders, J. Bastin, Mitochondrial trifunctional protein deficiency in human cultured fibroblasts: effects of bezafibrate, Journal of Inherited Metabolic Disease 39(1) (2016) 47-58.
[44] H. Li, S. Fukuda, Y. Hasegawa, H. Kobayashi, J. Purevsuren, Y. Mushimoto, S. Yamaguchi, Effect of heat stress and bezafibrate on mitochondrial β-oxidation: Comparison between cultured cells from normal and mitochondrial fatty acid oxidation disorder children using in vitro probe acylcarnitine profiling assay, Brain and Development 32(5) (2010) 362-370.
[45] U. Spiekerkoetter, Mitochondrial fatty acid oxidation disorders: clinical presentation of long-chain fatty acid oxidation defects before and after newborn screening, Journal of Inherited Metabolic Disease 33(5) (2010) 527-532.
[46] E.F. Diekman, S. Ferdinandusse, L. van der Pol, H.R. Waterham, J.P. Ruiter, L. Ijlst, R.J. Wanders, S.M. Houten, F.A. Wijburg, A.C. Blank, F.W. Asselbergs, R.H. Houtkooper, G. Visser, Fatty acid oxidation flux predicts the clinical severity of VLCAD deficiency, Genet Med (2015).
[47] S. Olpin, S. Clark, J. Dalley, B. Andresen, J. Croft, C. Scott, A. Khan, R. Kirk, R. Sparkes, M. Chard, A. Chan, E. Glamuzina, J. Bastin, N. Manning, R. Pollitt, Fibroblast Fatty-Acid Oxidation Flux Assays Stratify Risk in Newborns with Presumptive-Positive Results on Screening for Very-Long Chain Acyl-CoA Dehydrogenase Deficiency, International Journal of Neonatal Screening 3(1) (2017).
[48] J.C. Bleeker, I.L. Kok, S. Ferdinandusse, M. de Vries, T.G.J. Derks, M.F. Mulder, M. Williams, E. Rubio Gozalbo, A.M. Bosch, D.T. van den Hurk, M.G.M. de Sain-van der Velden, H.R. Waterham, F.A. Wijburg,

G. Visser, Proposal for an individualized dietary strategy in patients with very long-chain acyl-CoA dehydrogenase deficiency, Journal of Inherited Metabolic Disease (2018).
[49] T. Wang, M.J. Brown, mRNA Quantification by Real Time TaqMan Polymerase Chain Reaction: Validation and Comparison with RNase Protection, Analytical Biochemistry 269(1) (1999) 198-201.
[50] S.A. Bustin, Absolute quantification of mRNA using real-time reverse transcription polymerase chain reaction assays, Journal of Molecular Endocrinology 25(2) (2000) 169-193.
[51] H. Towbin, T. Staehelin, J. Gordon, Electrophoretic transfer of proteins from polyacrylamide gels to nitrocellulose sheets: procedure and some applications, Proceedings of the National Academy of Sciences of the United States of America 76(9) (1979) 4350-4354.
[52] G.M. Aldridge, D.M. Podrebarac, W.T. Greenough, I.J. Weiler, The use of total protein stains as loading controls: An alternative to high-abundance single-protein controls in semi-quantitative immunoblotting, Journal of Neuroscience Methods 172(2) (2008) 250-254.
[53] A.J. Duncan, I.P. Hargreaves, M.S. Damian, J.M. Land, S.J. Heales, Decreased ubiquinone availability and impaired mitochondrial cytochrome oxidase activity associated with statin treatment, Toxicol Mech Methods 19(1) (2009) 44-50.
[54] D. Shepherd, P.B. Garland, The kinetic properties of citrate synthase from rat liver mitochondria, Biochemical Journal 114(3) (1969) 597-610.
[55] O.H. Lowry, N.J. Rosebrough, A.L. Farr, R.J. Randall, Protein measurement with the folin phenol reagent, Journal of Biological Chemistry 193(1) (1951) 265-275.
[56] A.J.M. Janssen, F.J.M. Trijbels, R.C.A. Sengers, J.A.M. Smeitink, L.P. van den Heuvel, L.T.M. Wintjes, B.J.M. Stoltenborg-Hogenkamp, R.J.T. Rodenburg, Spectrophotometric Assay for Complex I of the Respiratory Chain in Tissue Samples and Cultured Fibroblasts, Clinical Chemistry 53(4) (2007) 729.
[57] P. Shelley, J. Tarry-Adkins, M. Martin-Gronert, L. Poston, S. Heales, J. Clark, S. Ozanne, J. McConnell, Rapid neonatal weight gain in rats results in a renal ubiquinone (CoQ) deficiency associated with premature death, Mechanisms of Ageing and Development 128(11) (2007) 681-687.
[58] S. Larsen, J. Nielsen, C.N. Hansen, L.B. Nielsen, F. Wibrand, N. Stride, H.D. Schroder, R. Boushel, J.W. Helge, F. Dela, M. Hey-Mogensen, Biomarkers of mitochondrial content in skeletal muscle of healthy young human subjects, The Journal of Physiology 590(Pt 14) (2012) 3349-3360.
[59] L. Canevari, S. Kuroda, T.E. Bates, J.B. Clark, B.K. Siesjö, Activity of Mitochondrial Respiratory Chain Enzymes after Transient Focal Ischemia in the Rat, Journal of Cerebral Blood Flow & Metabolism 17(11) (1997) 1166-1169.
[60] M.E. Skindersoe, M. Rohde, S. Kjaerulff, A novel and rapid apoptosis assay based on thiol redox status, Cytometry. Part A : the journal of the International Society for Analytical Cytology 81(5) (2012) 430-6.
[61] M.E. Skindersoe, S. Kjaerulff, Comparison of three thiol probes for determination of apoptosis-related changes in cellular redox status, Cytometry Part A 85(2) (2014) 179-187.
[62] P.R. Rich, A. Marechal, The mitochondrial respiratory chain, Essays Biochem 47 (2010) 1-23.
[63] M.D. Brand, The sites and topology of mitochondrial superoxide production, Experimental gerontology 45(7-8) (2010) 466-472.
[64] M. Akram, Citric Acid Cycle and Role of its Intermediates in Metabolism, Cell Biochemistry and Biophysics 68(3) (2014) 475-478.
[65] A.-C.M.F. Martines, K. van Eunen, D.-J. Reijngoud, B.M. Bakker, The promiscuous enzyme medium-chain 3-keto-acyl-CoA thiolase triggers a vicious cycle in fatty-acid beta-oxidation, PLOS Computational Biology 13(4) (2017) e1005461.
[66] K. van Eunen, S.M. Simons, A. Gerding, A. Bleeker, G. den Besten, C.M. Touw, S.M. Houten, B.K. Groen, K. Krab, D.J. Reijngoud, B.M. Bakker, Biochemical competition makes fatty-acid beta-oxidation vulnerable to substrate overload, PLoS Comput Biol 9(8) (2013) e1003186.

[67] U. Spiekerkoetter, M. Mueller, M. Sturm, M. Hofmann, D.T. Schneider, Lethal Undiagnosed Very Long-Chain Acyl-CoA Dehydrogenase Deficiency with Mild C14-Acylcarnitine Abnormalities on Newborn Screening, JIMD reports 6 (2012) 113-115.
[68] T. Aoyama, I. Yazawa, H. Sugie, Y. Shigematsu, N. Sakura, H. Nakase, [A case of skeletal muscle type very-long-chain-acyl CoA dehydrogenase(VLCAD) deficiency with repeated rhabdomyolysis], No To Shinkei 56(1) (2004) 64-68.
[69] S. Dey, A. Sidor, B. O'Rourke, Compartment-specific Control of Reactive Oxygen Species Scavenging by Antioxidant Pathway Enzymes, The Journal of biological chemistry 291(21) (2016) 11185-97.
[70] W. Dröge, Free Radicals in the Physiological Control of Cell Function, Physiological Reviews 82(1) (2002) 47-95.
[71] N.V. Dudkina, R. Kouřil, K. Peters, H.-P. Braun, E.J. Boekema, Structure and function of mitochondrial supercomplexes, Biochimica et Biophysica Acta (BBA) - Bioenergetics 1797(6–7) (2010) 664-670.
[72] S. Cogliati, J.A. Enriquez, L. Scorrano, Mitochondrial Cristae: Where Beauty Meets Functionality, Trends in Biochemical Sciences 41(3) (2016) 261-273.
[73] Y. Wang, A.-W. Mohsen, S.J. Mihalik, E.S. Goetzman, J. Vockley, Evidence for Physical Association of Mitochondrial Fatty Acid Oxidation and Oxidative Phosphorylation Complexes, Journal of Biological Chemistry 285(39) (2010) 29834-29841.
[74] J. Nouws, H. te Brinke, L.G. Nijtmans, S.M. Houten, ACAD9, a complex I assembly factor with a moonlighting function in fatty acid oxidation deficiencies, Human Molecular Genetics 23(5) (2014) 1311-1319.
[75] M. Schiff, B. Haberberger, C. Xia, A.-W. Mohsen, E.S. Goetzman, Y. Wang, R. Uppala, Y. Zhang, A. Karunanidhi, D. Prabhu, H. Alharbi, E.V. Prochownik, T. Haack, J. Häberle, A. Munnich, A. Rötig, R.W. Taylor, R.D. Nicholls, J.-J. Kim, H. Prokisch, J. Vockley, Complex I assembly function and fatty acid oxidation enzyme activity of ACAD9 both contribute to disease severity in ACAD9 deficiency, Human Molecular Genetics 24(11) (2015) 3238-3247.
[76] M. Pawlak, P. Lefebvre, B. Staels, Molecular mechanism of PPARα action and its impact on lipid metabolism, inflammation and fibrosis in non-alcoholic fatty liver disease, Journal of Hepatology 62(3) (2015) 720-733.
[77] H.-H. Chen, Y.-M. Sue, C.-H. Chen, Y.-H. Hsu, C.-C. Hou, C.-Y. Cheng, S.-L. Lin, W.-L. Tsai, T.-W. Chen, T.-H. Chen, Peroxisome proliferator-activated receptor alpha plays a crucial role in l -carnitine anti-apoptosis effect in renal tubular cells, Nephrology Dialysis Transplantation 24(10) (2009) 3042-3049.
[78] D. Giuseppe, S. Amirhossein, M. Pamela, The role of various peroxisome proliferator-activated receptors and their ligands in clinical practice, Journal of cellular physiology 233(1) (2018) 153-161.
[79] W. Wang, J. Palmfeldt, A.-W. Mohsen, N. Gregersen, J. Vockley, Fasting induces prominent proteomic changes in liver in very long chain Acyl-CoA dehydrogenase deficient mice, Biochemistry and biophysics reports 8 (2016) 333-339.
[80] N. Bujan, A. Arias, R. Montero, J. Garcia-Villoria, W. Lissens, S. Seneca, C. Espinos, P. Navas, L. De Meirleir, R. Artuch, P. Briones, A. Ribes, Characterization of CoQ(1)(0) biosynthesis in fibroblasts of patients with primary and secondary CoQ(1)(0) deficiency, Journal of inherited metabolic disease 37(1) (2014) 53-62.
[81] I. Pravst, K. Žmitek, J. Žmitek, Coenzyme Q10 Contents in Foods and Fortification Strategies, Critical Reviews in Food Science and Nutrition 50(4) (2010) 269-280.
[82] A.V. Berezhnov, E.I. Fedotova, M.N. Nenov, Y.M. Kokoz, V.P. Zinchenko, V.V. Dynnik, Destabilization of the cytosolic calcium level and the death of cardiomyocytes in the presence of derivatives of long-chain fatty acids, Biophysics 53(6) (2008) 564-570.
[83] S.C. Ley, L.P.S. de Carvalho, Protein CoAlation: a redox-linked post-translational modification, The Biochemical journal 474(16) (2017) 2897-2899.

[84] M.H. Stipanuk, J.J.E. Dominy, J.-I. Lee, R.M. Coloso, Mammalian Cysteine Metabolism: New Insights into Regulation of Cysteine Metabolism, The Journal of Nutrition 136(6) (2006) 1652S-1659S.
[85] C. Lind, R. Gerdes, Y. Hamnell, I. Schuppe-Koistinen, H.B. von Löwenhielm, A. Holmgren, I.A. Cotgreave, Identification of S-glutathionylated cellular proteins during oxidative stress and constitutive metabolism by affinity purification and proteomic analysis, Archives of Biochemistry and Biophysics 406(2) (2002) 229-240.
[86] P. Schönfeld, L. Wojtczak, Fatty acids as modulators of the cellular production of reactive oxygen species, Free Radical Biology and Medicine 45(3) (2008) 231-241.
[87] L.F. Ferreira, O. Laitano, REGULATION OF NADPH OXIDASES IN SKELETAL MUSCLE, Free radical biology & medicine 98 (2016) 18-28.
[88] Z.T. Schug, E. Gottlieb, Cardiolipin acts as a mitochondrial signalling platform to launch apoptosis, Biochimica et Biophysica Acta (BBA) - Biomembranes 1788(10) (2009) 2022-2031.
[89] S.M. Claypool, C.M. Koehler, The complexity of cardiolipin in health and disease, Trends in Biochemical Sciences 37(1) (2012) 32-41.
[90] J.F. Turrens, Mitochondrial formation of reactive oxygen species, The Journal of Physiology 552(2) (2003) 335-344.
[91] S. Vesce, M.B. Jekabsons, L.I. Johnson-Cadwell, D.G. Nicholls, Acute Glutathione Depletion Restricts Mitochondrial ATP Export in Cerebellar Granule Neurons, Journal of Biological Chemistry 280(46) (2005) 38720-38728.
[92] V. Lysne, E. Strand, G.F.T. Svingen, B. Bjørndal, E.R. Pedersen, Ø. Midttun, T. Olsen, P.M. Ueland, R.K. Berge, O. Nygård, Peroxisome Proliferator-Activated Receptor Activation is Associated with Altered Plasma One-Carbon Metabolites and B-Vitamin Status in Rats, Nutrients 8(1) (2016) 26.
[93] M. Moulin, A. Ferreiro, Muscle redox disturbances and oxidative stress as pathomechanisms and therapeutic targets in early-onset myopathies, Seminars in Cell & Developmental Biology 64 (2017) 213-223.
[94] K. Watanabe, S. Oda, A. Matsubara, S. Akai, T. Yokoi, Establishment and characterization of a mouse model of rhabdomyolysis by coadministration of statin and fibrate, Toxicol Lett 307 (2019) 49-58.
[95] U. Abshagen, S. Spörl-Radun, J. Marinow, Steady-state kinetics of bezafibrate and clofibrate in healthy female volunteers, European Journal of Clinical Pharmacology 17(4) (1980) 305-308.
[96] E. Kanterewicz, R. Sanmartí, J. Riba, I. Trias, J. Autonell, J. Brugués, Bezafibrate induced rhabdomyolysis, Annals of the Rheumatic Diseases 51(4) (1992) 536-538.
[97] K. Yamada, K. Tsunoda, K. Kawai, T. Ikeda, K. Taguchi, K. Kajita, H. Morita, T. Ishizuka, Mitochondria toxicity of antihyperlipidemic agents bezafibrate and fenofibrate, Diabetol Int 4(2) (2013) 126-131.
[98] B. Qu, Q.-T. Li, K.P. Wong, T.M.C. Tan, B. Halliwell, Mechanism of clofibrate hepatotoxicity: mitochondrial damage and oxidative stress in hepatocytes, Free Radical Biology and Medicine 31(5) (2001) 659-669.
[99] Q. Zhang, M. Raoof, Y. Chen, Y. Sumi, T. Sursal, W. Junger, K. Brohi, K. Itagaki, C.J. Hauser, Circulating mitochondrial DAMPs cause inflammatory responses to injury, Nature 464(7285) (2010) 104-7.
[100] K.R. Atkuri, J.J. Mantovani, L.A. Herzenberg, L.A. Herzenberg, N-Acetylcysteine—a safe antidote for cysteine/glutathione deficiency, Current Opinion in Pharmacology 7(4) (2007) 355-359.
[101] M. Kelly-Aubert, S. Trudel, J. Fritsch, T. Nguyen-Khoa, M. Baudouin-Legros, S. Moriceau, L. Jeanson, F. Djouadi, C. Matar, M. Conti, M. Ollero, F. Brouillard, A. Edelman, GSH monoethyl ester rescues mitochondrial defects in cystic fibrosis models, Human Molecular Genetics 20(14) (2011) 2745-2759.
[102] G. Leipnitz, A.W. Mohsen, A. Karunanidhi, B. Seminotti, V.Y. Roginskaya, D.M. Markantone, M. Grings, S.J. Mihalik, P. Wipf, B. Van Houten, J. Vockley, Evaluation of mitochondrial bioenergetics, dynamics, endoplasmic reticulum-mitochondria crosstalk, and reactive oxygen species in fibroblasts from patients with complex I deficiency, Scientific reports 8(1) (2018) 1165.

[103] K.-i. Tanaka, I. Miyazaki, N. Fujita, M.E. Haque, M. Asanuma, N. Ogawa, Molecular Mechanism in Activation of Glutathione System by Ropinirole, a Selective Dopamine D2 Agonist, Neurochemical Research 26(1) (2001) 31-36.
[104] F.-Z. Boufroura, C. Le Bachelier, C. Tomkiewicz-Raulet, D. Schlemmer, J.-F. Benoist, P. Grondin, Y. Lamotte, O. Mirguet, S. Mouillet-Richard, J. Bastin, F. Djouadi, A new AMPK activator, GSK773, corrects fatty acid oxidation and differentiation defect in CPT2-deficient myotubes, Human Molecular Genetics 27(19) (2018) 3417-3433.